along the Si–O bonds of the ZSM-5 framework [42].

In the embedded cluster model, the static Madelung potential due to atoms outside of the quantum cluster was represented by partial atomic charges located at the zeolite lattice sites. Using an approach recently proposed by Stefanovich and Truong [37], charges close to the quantum cluster are treated explicitly while the Madelung potential from the remaining charges from an infinite lattice is represented by a set of surface charges that were derived from the surface charge representation of external electrostatic potential (SCREEP) method. More details on this method can be found elsewhere [37]. In this study, the total Madelung potential is represented by 201 explicit charges within 3.5 Å to the quantum cluster and 688 surface charges. With this small number of point charges, additional computational cost is often less than 5% compared to bare cluster calculations.

Geometry optimizations were done at the HF level using the 6–31G(d,p) basis set. For embedded cluster models, capped hydrogen atoms were fixed along the Si–O bond during these optimizations. For CO adsorption on H-ZSM5 and Li-ZSM5, two possible adsorption configurations were investigated. One is called C-bound where CO approaches to the zeolite with the C-end. Similarly, the O-bound complex means the O-end approaching the zeolite. Geometries of these complexes are fully optimized without additional constraints besides those of the capped hydrogen atoms. The Gaussian 94 program [43] was used to carried out embedded cluster calculations whereas the TURBOMOLE program [44,45] for bare cluster calculations.

3. Results and discussion

3.1. Structure of H-ZSM-5 and Li-ZSM-5 zeolites

First, we examine the structure of the H-ZSM-5 zeolite. Cluster and embedded cluster

Table 1
HF/6–31G** optimized geometrical parameters of the H-ZSM-5 and H-ZSM-5/CO systems (bond lengths are in Å and bond angles in degrees)

	H-ZSM-5		H-ZSM-5/CO			
	Bare cluster	Embedded cluster	Bare cluster		Embedded cluster	
			C-bound	O-bound	C-bound	O-bound
Al–H_b	2.326	2.338	2.343	2.337	2.352	2.342
O_2–H_b	0.946	0.953	0.953	0.951	0.960	0.956
Al–O_1	1.681	1.678	1.684	1.681	1.680	1.678
Al–O_2	1.866	1.859	1.861	1.863	–	–
Si_2–O_2	1.688	1.685	1.684	1.685	1.678	1.680
Si_1–O_1	1.605	1.587	1.604	1.602	1.585	1.584
C–O	–	–	1.111	1.115	1.110	1.116
H_b–C	–	–	2.230	–	2.184	–
H_b–O	–	–	–	2.147	–	2.028
O_1–Al–O_2	93.0	94.8	93.5	93.4	95.6	95.6
Si_2–O_2–Al	135.2	135.2	134.9	134.9	135.3	135.4
H_b–O_2–O_1–Al	181.2	177.6	183.9	183.1	179.8	178.8
Si_1–O_1–Al–O_2	161.1	160.0	160.4	160.1	158.9	158.7
Si_2–O_2–Al–O_1	181.5	181.4	181.3	180.8	180.8	180.7
C–O_2–O_1–Al			186.4		182.5	
O–O_2–O_1–Al				185.9		180.8
q(H)	0.415	0.435	0.436	0.441	0.454	0.464
q(O_1)	−0.914	−0.884	−0.924	−0.912	−0.886	−0.882
q(O_2)	−0.802	−0.805	−0.835	−0.824	−0.843	−0.832

models for this zeolite are shown in Fig. 1. Selected optimized geometrical parameters and partial charges at the Brønsted site are listed in Table 1. Comparing results between cluster and embedded cluster models, the Madelung potential has an effect of elongating the O_2–H_b bond distance (Brønsted acid site) less than 0.01 Å and increasing the positive charge on H_b atom by 0.02 AU, thus, enhancing the acidity of the Brønsted acid site. Our results are similar to those obtained by Greatbanks et al. [38] using a different embedded cluster approach with potential derived charges. The calculated Al–H_b distance of 2.338 Å from the embedded cluster model is also consistent with the NMR measurement of 2.38 ± 0.04 Å [46]. As noted above, the Madelung potential was found to also lengthen the Al–H_b distance by about 0.01 Å. This is within the uncertainty of the experimental data. Thus, the Madelung field has a small effect on the structure of the Brønsted site. However, it was found to have a larger effect on the energetic properties as discussed below.

For the Li-ZSM-5 zeolite (see Fig. 2), the Li cation does not bind to a particular bridging oxygen atom but rather symmetrically bidentates to O_1 and O_2 atoms of the [AlO_4] tetrahedron as confirmed by an ESR experiment [47]. Geometrical parameters of the Li-ZSM5 are listed in Table 2. The bare cluster calculations predict the Li cation to be out of the (O_2, Al, O_1) plane by 5° in the Li–O_2–O_1–Al dihedral angle. The Madelung potential brings the cation to within 1° in this dihedral angle from being in

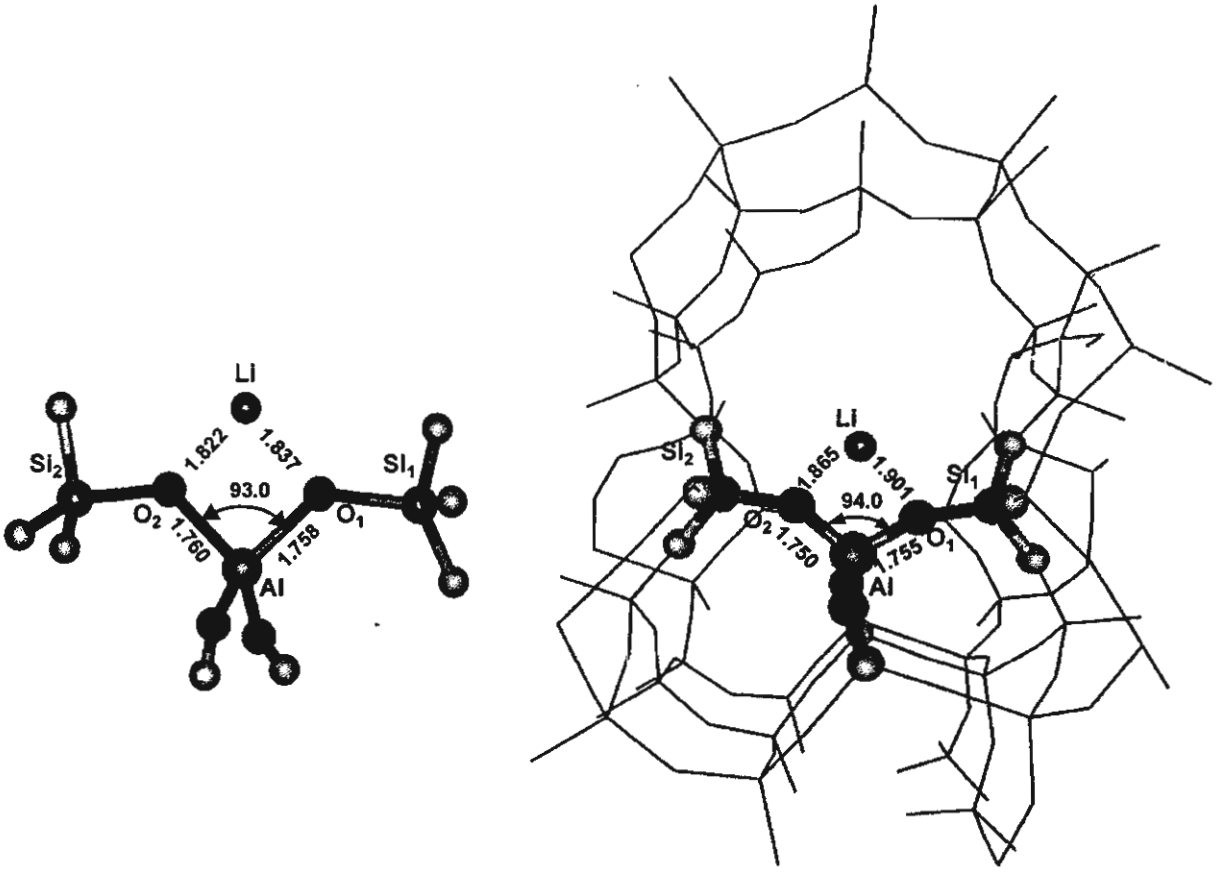

Fig. 2. Similar to Fig. 1, but for the Li-ZSM-5 zeolite.

Table 2
HF/6–31G** optimized geometrical parameters of the Li-ZSM-5 and Li-ZSM-5/CO systems (bond lengths are in Å and bond angles in degrees)

	Li-ZSM-5		Li-ZSM-5/CO			
	Bare cluster	Embedded cluster	Bare cluster		Embedded cluster	
			C-bound	O-bound	C-bound	O-bound
Li–Al	2.519	2.573	2.533	2.535	2.588	2.583
Li–O_1	1.837	1.901	1.851	1.852	1.920	1.914
Li–O_2	1.822	1.865	1.832	1.837	1.874	1.875
Al–O_1	1.758	1.755	1.755	1.755	1.753	1.752
Al–O_2	1.760	1.750	1.757	1.757	1.747	1.747
Si–O_2	1.626	1.617	1.623	1.623	1.614	1.614
Si–O_1	1.624	1.607	1.621	1.620	1.606	1.605
CO	–	–	1.107	1.118	1.109	1.117
Li–C	–	–	2.343	–	2.353	–
Li–O	–	–	–	2.078	–	2.064
O_1–Li–O_2	88.4	85.8	87.7	87.5	85.1	85.3
O_1–Al–O_2	93.0	94.0	93.2	93.2	94.3	94 3
Si–O_2–Al	130.1	131.4	130.3	130.3	131.7	131.7
Li–O_2–O_1–Al	185.1	178.6	184.4	185.1	178.5	178.6
Si_1–O_1–Al–O_2	160.7	162.2	160.8	160.7	161.7	161.6
Si_2–O_2–Al–O_1	182.4	181.8	182.0	182.2	181.7	181.9
C–O_2–O_1–Al	–	–	183.1	–	183.2	–
O–O_2–O_1–Al	–	–	–	183.6	–	183.7
q(Li^+)	0.666	0.719	0.515	0.609	0.570	0.658
q(O_1)	−1.011	−0.991	−1.011	−1.013	−0.991	−0.993
q(O_2)	−1.011	−0.999	−1.011	−1.012	−0.998	−0.999

the same plane. However, the interaction of Li cation with zeolite leads to substantial perturbation on the zeolite framework near the active site. In particular, comparing the embedded cluster results listed in Tables 1 and 2 for H-ZSM5 and Li-ZSM-5 systems, we found the Al–O_2 distance is shorten by 0.109 Å while the other Al–O_1 distance is elongated by 0.077 Å; similarly, the Si–O_2 bond shorten by 0.068 Å while the Si–O_1 bond elongated by 0.02 Å; but the O_1–Al–O_2 angle has no significant change upon metal exchange. In a reciprocal effect, the zeolite framework reduces the Li cation charge to 0.72 AU. The Madelung potential was found to have a larger effect on the structure of Li-ZSM-5 zeolite. Particularly, it elongates the Al–Li distance by 0.54 Å and decreases the O_1–Li–O_2 angle by 2.6°. This indicates the Madelung field weakening the attachment of the Li cation to the zeolite framework. One can expect that in this case, adsorption on the Li-ZSM-5 will be affected by the presence of the Madelung potential.

3.2. Adsorption of CO on H-ZSM-5 and Li-ZSM-5 zeolites

Cluster and embedded cluster models for the adsorption of CO on H-ZSM-5 and Li-ZSM-5 zeolites are illustrated in Figs. 3 and 4, respectively. Selected geometrical parameters of the adduct complexes are listed in Tables 1 and 2. Adsorption energies calculated by using different models are given in Table 3.

We found that adsorption of CO does not affect the zeolite framework significantly. Though this can be expected due to the small dipole of CO. The geometry of the H-ZSM-5 or Li-ZSM-5 Brønsted site changes by at most 0.01 Å for bond distances and 1° for angles due to CO adsorption. This result has an important implication that is in future theoretical studies

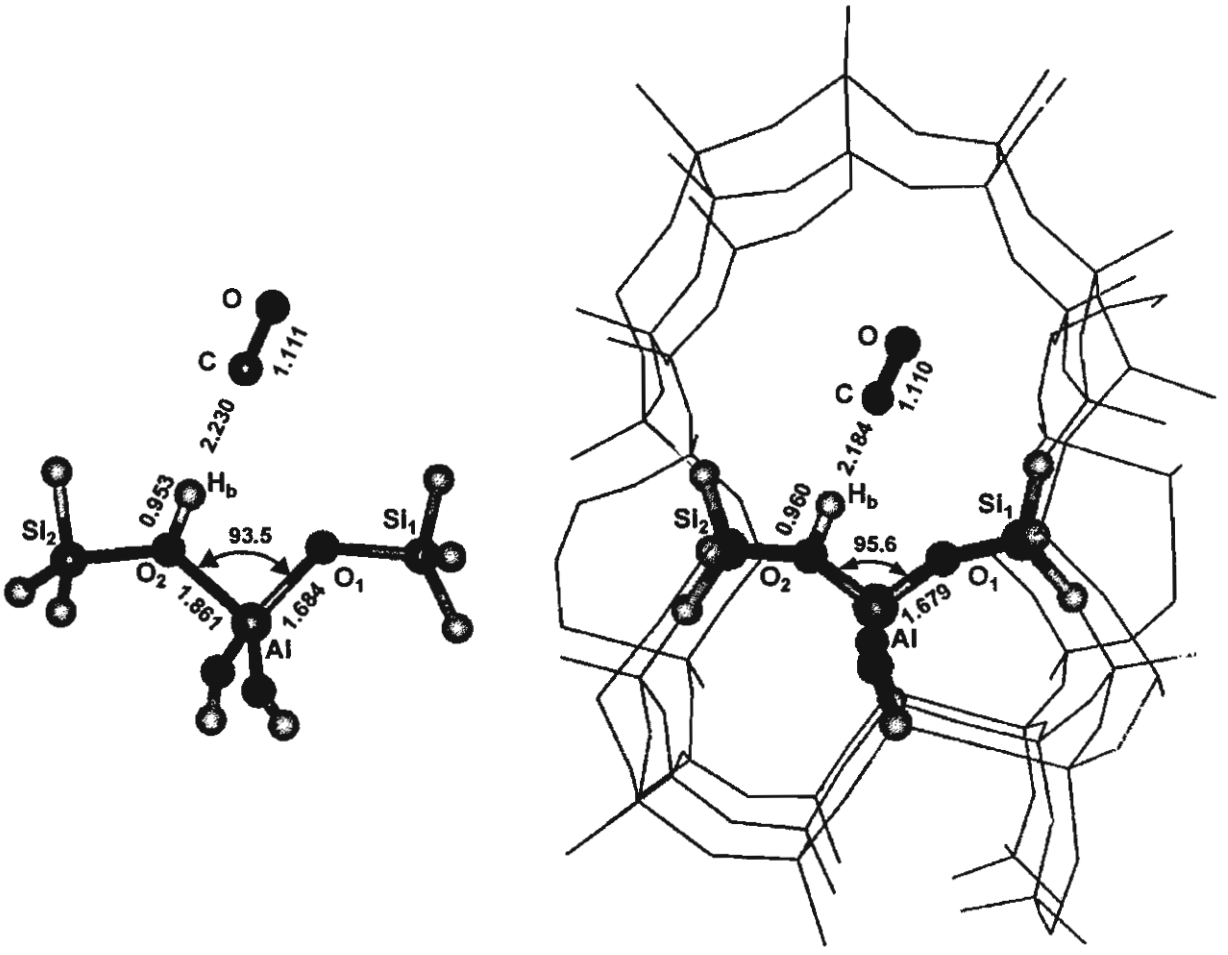

Fig. 3. Similar to Fig. 1, but for the H-ZSM-5/CO complex.

of adsorption of similar species, it is possible without loosing much accuracy to fix the zeolite framework in optimization of the complex structure. This would accelerate the convergence and reduce significantly the computational cost.

For the C-bound complex on H-ZSM-5, the distance from the C atom to the Brønsted proton was predicted to be 2.230 Å using the cluster model. Including the Madelung potential shortens this distance by 0.046 Å. The effect is noticeably smaller for adsorption on Li-ZSM-5. It is interesting to note that adsorption of CO increases the charge of the Brønsted acid proton by more than 0.02 AU whereas it decrease the Li cation charge by as large as 0.15 AU.

The effects of the Madelung potential are more profound in the adsorption energies of CO on both H-ZSM-5 and Li-ZSM-5 as listed in Table 3. For the adsorption of CO on H-ZSM-5 zeolite, we found that both bare cluster and embedded cluster models predict both C-bound and O-bound adducts existed with the C-bound being more stable by 1 kcal/mol. For adsorption of CO on Li-ZSM-5 zeolite, C-bound and O-bound complexes have almost the same binding energy within the uncertainty of the calculations. We found that the Madelung potential increases the binding energy by 2.5 kcal/mol in the H-ZSM-5 and 3.0 kcal/mol in the Li-ZSM-5 zeolite. With inclusion of basis-set superposi-

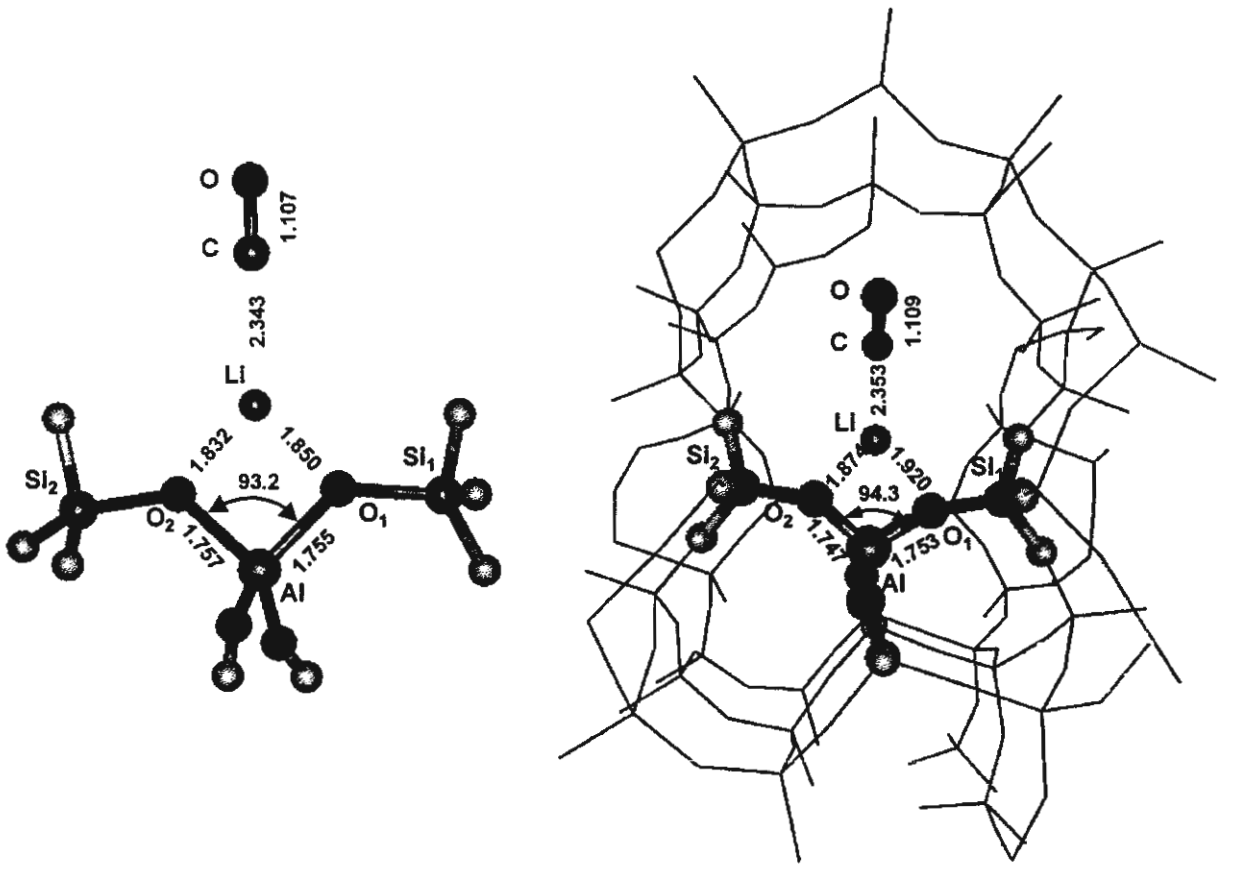

Fig. 4. Similar to Fig. 1, but for the Li-ZSM-5/CO complex.

tion error (BSSE) correction calculated using the counterpoise correction method and effects of Madelung potential, we predict that CO adsorbs on H-ZSM-5 zeolite in a C-bound complex preferably with a binding energy of 4.95 kcal/mol. This is in consistent with the experimental range of 3.25–4.10 kcal/mol obtained by Gupta et al. [48] for a lower acidic zeolite H–X using a range of acidic site compositions. For Li-ZSM-5 zeolites, both adducts exist with the C-bound configuration being slightly more stable and having the binding energy of 8.56 kcal/mol. Again this is in reasonable agreement with the binding energy of 6.7 kcal/mol for

Table 3
Calculated adsorption energies (kcal/mol) of CO on naked Li(I), bare quantum cluster and embedded cluster model of H-ZSM-5 and Li-ZSM-5 zeolites

	Naked		Embedded		3T quantum cluster		Embedded		3T quantum cluster	
	Li/CO	Li/OC	Li-ZSM-5 /CO	Li-ZSM-5 /OC	Li-ZSM-5 /CO	Li-ZSM-5 /OC	HZSM-5 /CO	HZSM-5 /OC	HZSM-5 /CO	HZSM-5 /OC
ΔE	−14.62	−16.44	−10.78	−10.38	−8.04	−7.90	−6.09	−4.75	−3.61	−2.26
ΔE(BSSE)	−13.14	−15.25	−8.56	−8.03	−5.77	−5.56	−4.95	−3.62	−2.25	−1.41

adsorption of CO on Na–Y zeolite [49]. Since Na^+ is larger than Li^+, one can expect that CO would bind more strongly to Li-ZSM-5 than Na-ZSM-5. It is interesting to compare the adsorption of CO on Li-ZSM-5 zeolite with the case where the zeolite framework is absent, i.e., in the naked Li^+–CO system. The adsorption energies for both C-bound and O-bound Li^+–CO complexes are also listed in Table 3. As expected, the CO binds much more strongly to the Li^+ cation than in the Li-ZSM-5 zeolite by almost a factor of 2 in the binding energy. An interesting result is that the O-bound complex is more stable by about 2.11 kcal/mol compared to the C-bound complex in the Li^+–CO system. Thus, interactions with the ZSM-5 zeolite framework reverse the order of relative stability of these complexes.

4. Conclusions

The interaction of carbon monoxide (via the C-bound and O-bound adducts) with the H-ZSM-5 and metal-exchanged Li-ZSM-5 zeolites has been investigated by using both the quantum cluster and embedded cluster approaches. For both the H-ZSM-5 and Li-ZSM-5 zeolites, the C-bound adducts were found to be more stable than the O-bound adducts. Inclusion of the Madelung potential from the zeolite framework was found to noticeably increase on the binding energies of these adducts and leads to better agreement with experimental observation. The results obtained in this study also suggested that the embedded cluster approach provides a more accurate and practical model than the bare cluster one for studying zeolite structure and catalytic activity.

Acknowledgements

This work was supported by donors of the Thailand Research Fund (TRF) in supporting the research career development project (The TRF Research Scholar) and the Kasetsart University Research and Development Institute (KURDI) to J.L. T.N.T. acknowledges the support from the National Science Foundation (CHE-9817918). We also thank Professor R. Ahlrichs (Karlsruhe, Germany) for his continued support of this work.

References

[1] J. Klinowski, Chem. Rev. 91 (1991) 1459.
[2] J.M. Thomas, Sci. Am. 266 (1992) 82.
[3] G.J. Kramer, R.A. van Santen, C.A. Emeis, A.K. Nowak, Nature 363 (1993) 529.
[4] E. Kassab, J. Fouquet, M. Allavena, E.M. Evleth, J. Phys. Chem. 97 (1993) 9034.
[5] C.T.W. Chu, C.D. Chang, J. Phys. Chem. 89 (1985) 1569.
[6] M.A. Makarova, S.P. Bates, J. Dwyer, J. Am. Chem. Soc. 117 (1995) 11309.
[7] J. Das, C.V.V. Satyanaryana, D.K. Chakrabarty, S.N. Piramanayagam, S.N. Shringi, J. Chem. Soc., Faraday Trans. 88 (1992) 3255.
[8] S.R. Blaszkowski, R.A. van Santen, J. Phys. Chem 99 (1995) 11728.
[9] H.J. Soscun, P.J. Omalley, A. Hinchliffe, J. Mol Struct.: THEOCHEM 341 (1995) 237.
[10] J. Limtrakul, S. Pollman-Hannongbua, J. Mol. Struct.: THEOCHEM 280 (1993) 139.
[11] J. Limtrakul, J. Mol. Struct. 288 (1993) 105.
[12] J. Limtrakul, Chem. Phys. 193 (1995) 79.
[13] J. Limtrakul, P. Treesakol, M. Probst, Chem. Phys. 215 (1997) 77.
[14] J. Limtrakul, U. Onthong, J. Mol. Struct. 435 (1997) 181.
[15] J. Limtrakul, D. Tantanak, J. Mol. Struct. 358 (1995) 179.
[16] J. Limtrakul, D. Tantanak, Chem. Phys. 208 (1996) 331.
[17] J.A. Zygmunt, L.A. Curtiss, L.E. Iton, M.K. Erhardt, J. Phys. Chem. 100 (1996) 6663.
[18] M. Krossner, J. Sauer, J. Phys. Chem. 100 (1996) 6199.
[19] F. Haase, J. Sauer, J. Am. Chem. Soc. 117 (1995) 3780.
[20] A.T. Bell, Catal. Today 38 (1997) 151.
[21] M. Katoh, T. Yamazaki, H. Kamijo, S. Ozawa, Zeolites 15 (1995) 591.
[22] H.V. Brand, A. Redondo, P.J. Hay, J. Phys. Chem. B 101 (1997) 7691.
[23] I.N. Senchenya, E. Garrone, P. Ugliengo, J. Mol. Struct.: THEOCHEM 368 (1996) 93.
[24] J. Sauer, P. Ugliengo, E. Garrone, V.R. Saunders, Chem. Rev. 94 (1994) 2095.
[25] P. Geerling, N. Tariel, A. Botrel, R. Lissillour, W.J. Morlier, J. Phys. Chem. 88 (1984) 5752.
[26] P. Ugliengo, V.R. Saunders, E. Garrone, J. Phys. Chem. 93 (1989) 5210.
[27] S. Bates, J. Dwyer, J. Phys. Chem. 97 (1993) 5897.
[28] K.M. Neyman, P. Strodel, S.Ph. Ruzankin, N. Schlensog, H. Knozinger, N. Rosch, Catal. Lett. 31 (1995) 273.

[29] S. Ikuta, Chem. Phys. 95 (1985) 235.
[30] S. Ikuta, Chem. Phys. 109 (1984) 550.
[31] A.M. Ferrari, P. Ugliengo, E. Garrone, J. Chem. Phys. 105 (1996) 4129.
[32] N.U. Zhanpeisov, H. Nakatsuji, M. Hada, H. Nakai, M. Anpo, Catal. Lett. 42 (1996) 173.
[33] K.C. Hass, W.F. Schneider, J. Phys. Chem. 100 (1996) 9292.
[34] W.F. Schneider, K.C. Hass, R. Ramprasad, J.B. Adams, J. Phys. Chem. 100 (1996) 6032.
[35] B.L. Trout, A.K. Chakraborty, A.T. Bell, J. Phys. Chem. 100 (1996) 4173.
[36] D.A. Dixon, J.L. Gole, A. Komornicki, J. Phys. Chem. 92 (1988) 1378.
[37] E.V. Stefanovich, T.N. Truong, J. Phys. Chem. B 102 (1998) 3018.
[38] S.P. Greatbanks, I.H. Hillier, N.A. Burton, P. Sherwood, J. Chem. Phys. 105 (1996) 3370.
[39] R. Dovesi, V.R. Saunders, C. Roetti, CRYSTAL 92, An ab initio Hartree-Fock LCAO Program for Periodic Systems, Theoretical Chemistry Group, University of Torino and SERC, Daresbury Laboratory, 1992.
[40] L. Campana, A. Selloni, J. Weber, A. Pasquarello, I. Papai, A. Goursot, Chem. Phys. Lett. 226 (1994) 245.
[41] E.H. Teunissen, C. Roetti, C. Pisani, A.J.M. de Man, A.P.J. Jansen, R. Orlando, R.A. van Santen, R. Dovesi, Modelling, Simul. Mater. Sci. Eng. 2 (1994) 921.
[42] H. van Koningsveld, H. Van Bekkum, J.C. Jansen, Acta Crystallogr. B 43 (1987) 127.
[43] M.J. Frisch, G.W. Trucks, H.B. Schlegel, P.M.W. Gill, B.G. Johnson, M.W. Wong, J.B. Foresman, M.A. Robb, M. Head-Gordon, E.S. Replogle, R. Gomperts, J.L. Andres, K. Raghavachari, I.S. Binkley, C. Gonzalez, R.L. Martin, D.J. Fox, D.J. DeFrees, J. Baker, J.J.P. Stewart, J.A. Pople, Gaussian 94, Gaussian, Pittsburgh, 1994.
[44] R. Ahlrichs, R. Baer, M. Haeser, H. Horn, C. Kölmel, Chem. Phys. Lett. 162 (1989) 165.
[45] M. Haeser, R. Ahlrichs, J. Comput. Chem. 10 (1989) 104.
[46] D. Freude, J. Klinowski, H. Hamdan, Chem. Phys. Lett. 149 (1988) 355.
[47] H. Hosono, H. Kawazoe, J. Nishii, J. Kanazawa, J. Non-Cryst. Solid 51 (1982) 217.
[48] N.M. Gupta, V.S. Kamble, A.K. Roa, R.M. Iyer, J. Catal. 120 (1989) 432.
[49] V. Bolis, B. Fubini, E. Garrone, E. Giamello, C. Morterra, in: C. Morterra, A. Zecchina, G. Costa (Eds.), Structure and Reactivity of Surfaces, Elsevier, Amsterdam, 1989.

ELSEVIER

Journal of Molecular Structure 525 (2000) 153–162

Journal of
MOLECULAR
STRUCTURE

www.elsevier.nl/locate/molstruc

Adsorption of carbon monoxide on H-FAU and Li-FAU zeolites: an embedded cluster approach

J. Limtrakul*, S. Jungsuttiwong, P. Khongpracha

Laboratory for Computational and Applied Chemistry, Chemistry Department, Faculty of Science, Kasetsart University, Bangkok 10900, Thailand

Received 25 October 1999; accepted 17 December 1999

Abstract

The interaction of carbon monoxide with H-faujasite (H-FAU) and metal-exchange Li-FAU zeolites has been investigated by means of cluster and embedded cluster approaches at the HF/6-31G(d,p) level of theory. In the case of the protonated zeolite, the adsorption energy of the bare quantum cluster is evaluated to be −1.90 kcal/mol for the H-FAU/CO complex. Inclusion of the Madelung potential field from the zeolite framework has an effect of lengthening the OH distance, hence enhancing the binding energies of the H-FAU/CO (−3.20 kcal/mol). For adsorption of CO on the metal-exchanged zeolites, the Madelung potential was found to differentiate the different types of zeolites (ZSM-5 and FAU), that cannot be drawn from the typical 3T-quantum cluster. This finding clearly demonstrates that acidity does not depend only on the Brønsted group center, but also on the dimension of the channel where the Brønsted group is located. The adsorption energy of the embedded cluster model (−6.69 kcal/mol) lies between those of the bare quantum cluster model (−5.81 kcal/mol) and the simple naked Li(I)/CO system (−13.14 kcal/mol). Correction of the 3T cluster model to take into account the long range contribution of the electrostatic potential of the zeolite crystal is found to agree with the experimental observation.

Keywords: Zeolite; Carbonmoxide; FAU; Embedded Cluster; Ab initio

1. Introduction

Zeolites are of prime importance as catalysts for many industrial processes, due mainly to their shape-selectivity and Brønsted acid sites [1–19]. Recently, metal-exchanged zeolites have been found to be potential catalysts for decomposition of NO_x and CO from automotive emission and power plants [20–22].

A review of quantum chemical calculations applied to zeolites and their interaction with carbon monoxide has been recently reported by Senchenya et al. [23]. All early works of adsorption CO on bare zeolite clusters were limited to the small model fragment $H_3SiOHAlH_3$, or 2T cluster, and are not specific to a particular zeolite, but represent a generic tetrahedral sub-unit in an unconstrained environment [23–36].

As is known, small zeolitic clusters may inadequately reflect adsorption complexes at the active site, and the cluster environment may enhance binding energy, and hence, accurately predict the structures of reaction intermediate, transition state and products.

In order to overcome the shortcomings in failing to take into account the electrostatic field in these solid acid catalysts, an embedded method has to be

* Corresponding author. Tel.: + 66-2-942-8034; fax: + 66-2-579-3955.

0022-2860/00/$ - see front matter
PII: S0022-2860(00)00423-3

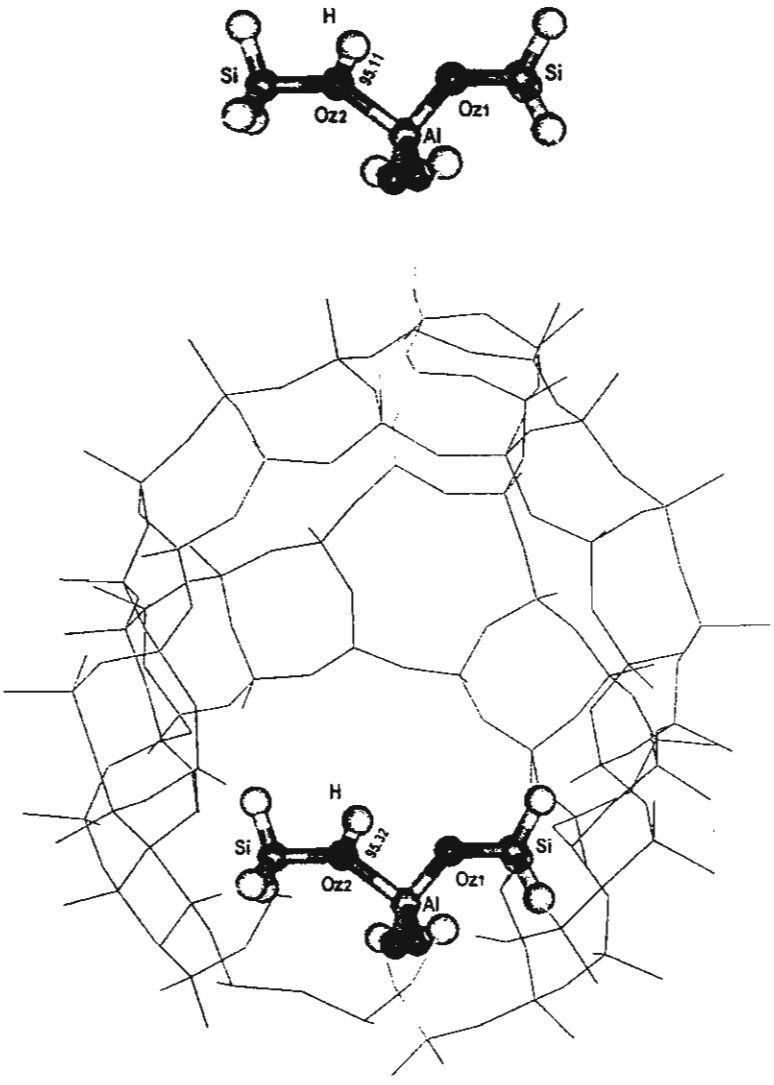

Fig. 1. Cluster and embedded cluster models of the H-FAU zeolite. Bond distances given in the figures are in pm.

employed [37,38]. To include the effects of the zeolite framework on adsorption of CO in zeolites, a periodic electrostatic structure method can be utilized [39–41]. This corresponds to the high loading case and is often computationally expensive for most zeolites due to their relatively large unit cells. Alternatively, the embedded cluster approach provides a more practical methodology with little additional computational cost, compared to the bare cluster calculation [37].

2. Method

We employed the clusters illustrated in Figs. 1–4 as the models of interaction of probe molecules on H-zeolites, and alkali-metal-exchanged zeolites $H_3SiO(X)Al(OH)_2OSiH_3$, and $H_3SiO(X)Al(OH)_2OSiH_3$/[CO], hereafter referred to as [H-FAU], [Li-FAU], [H-FAU]/[CO], and [Li-FAU]/[CO] respectively, where X is either H or Li atom. The naked alkali-cation/CO adducts, Li(I)/[CO], are also

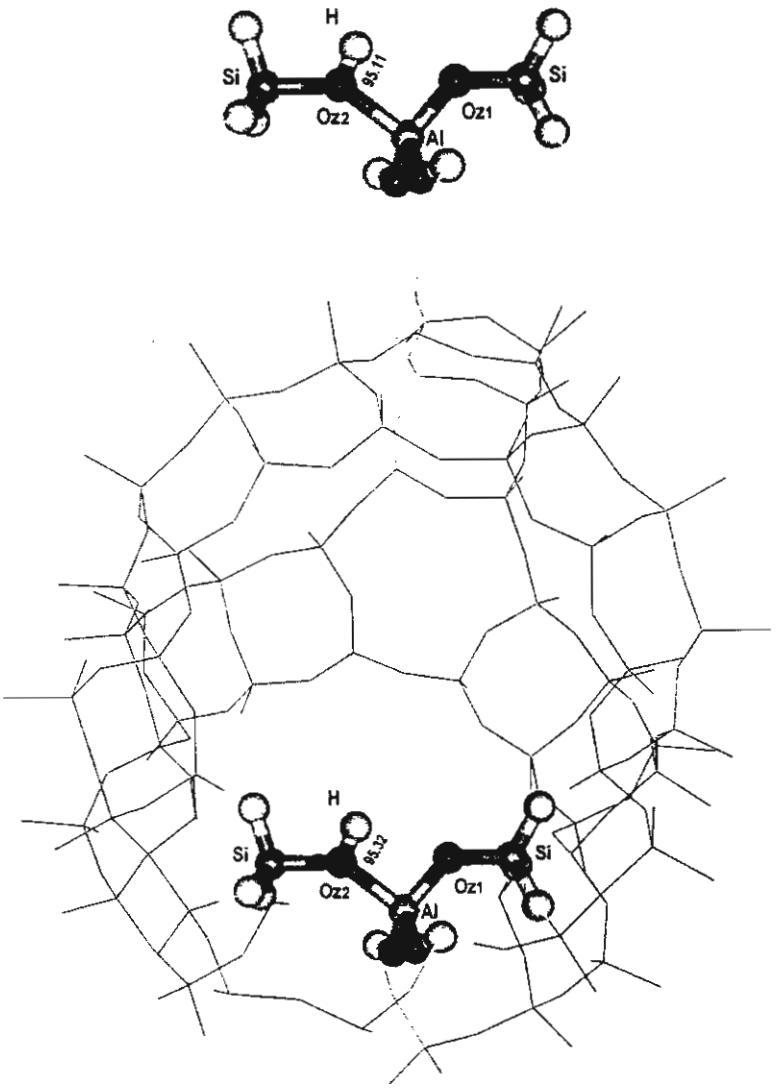

Fig. 1. Cluster and embedded cluster models of the H-FAU zeolite. Bond distances given in the figures are in pm.

employed [37,38]. To include the effects of the zeolite framework on adsorption of CO in zeolites, a periodic electrostatic structure method can be utilized [39–41]. This corresponds to the high loading case and is often computationally expensive for most zeolites due to their relatively large unit cells. Alternatively, the embedded cluster approach provides a more practical methodology with little additional computational cost, compared to the bare cluster calculation [37].

2. Method

We employed the clusters illustrated in Figs. 1–4 as the models of interaction of probe molecules on H-zeolites, and alkali-metal-exchanged zeolites $H_3SiO(X)Al(OH)_2OSiH_3$, and $H_3SiO(X)Al(OH)_2OSiH_3$/[CO], hereafter referred to as [H-FAU], [Li-FAU], [H-FAU]/[CO], and [Li-FAU]/[CO] respectively, where X is either H or Li atom. The naked alkali-cation/CO adducts, Li(I)/[CO], are also

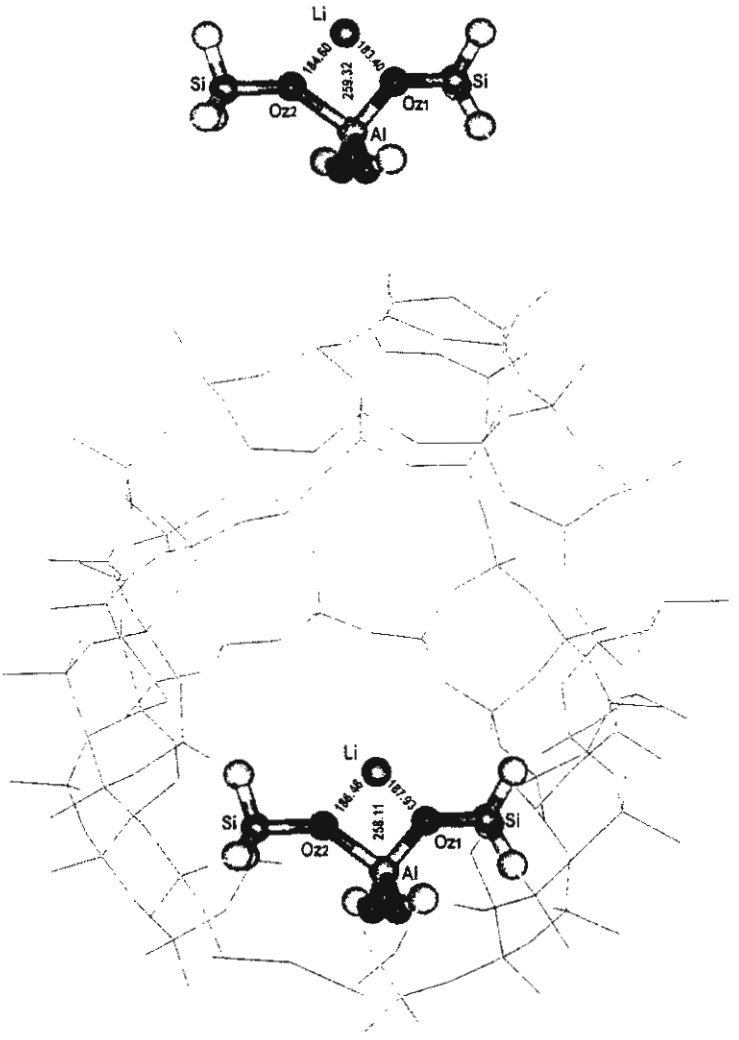

Fig. 2. Cluster and embedded cluster models of the Li-FAU zeolite. Bond distances given in the figures are in pm.

included for comparing with the effect of the negative zeolite oxygen framework surrounding the alkali cations.

The bare quantum clusters are selected to model specifically to faujasite zeolite. In these models, the dangling bonds of the Si atoms are terminated by H atoms and the Si–H bonds are aligned with the corresponding S–O bonds of the structures of faujasite zeolite, respectively [42].

In the embedded cluster model, the static Madelung potential due to atoms outside of the quantum cluster was represented by partial atomic charges located at the zeolite lattice sites. Using an approach recently proposed by Stefanovich and Troung [37], charges close to the quantum cluster are treated explicitly, while the Madelung potential from the remaining charges from an infinite lattice is represented by a set of surface charges that were derived from the Surface Charge Representation of External Electrostatic Potential (SCREEP) method. More details on this method can be found elsewhere [37]. In this study, the total Madelung potential is represented by 1137 explicit charges within 3.5 Å to the quantum cluster and 146 surface charges. With this small number of point charges,

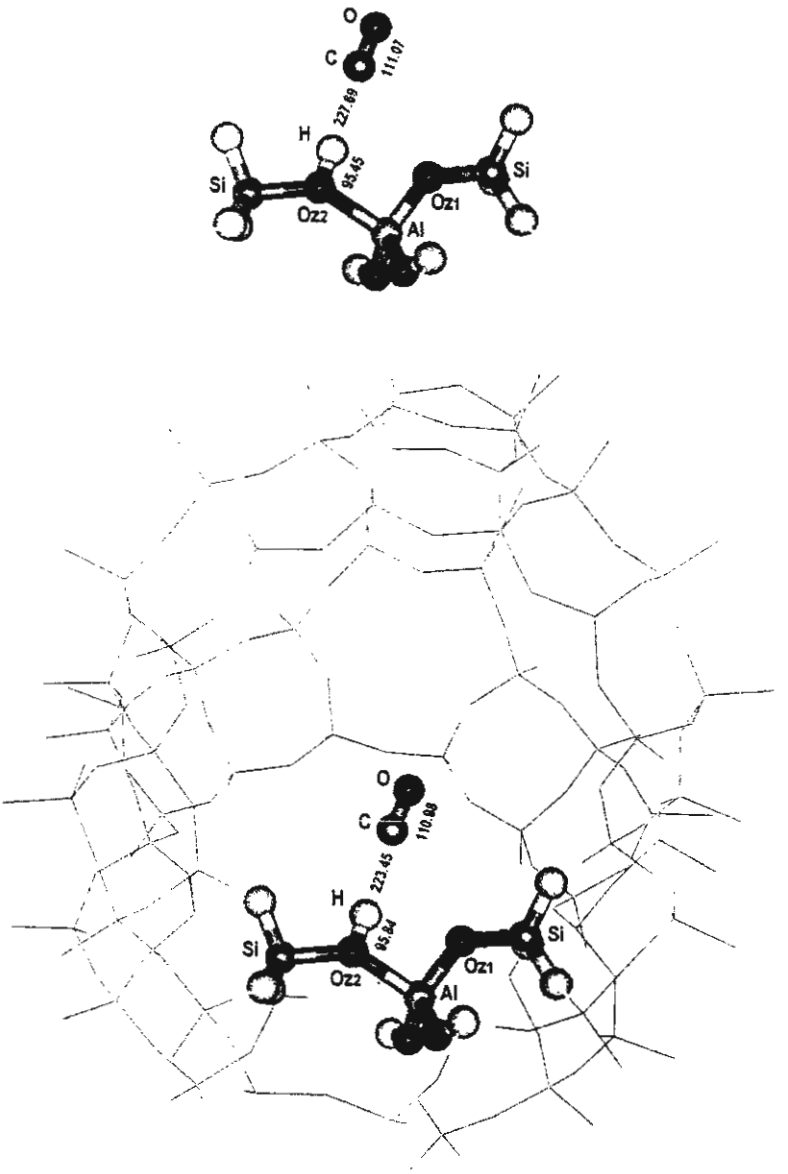

Fig. 3. Cluster and embedded cluster models of the H-FAU/CO complex. Bond distances given in the figures are in pm.

additional computational cost is often less than 5% compared to bare cluster calculations.

Geometry optimizations were done at the HF level using 6-31G(d,p) basis. The GAUSSIAN94 program [43] was employed to carry out embedded cluster calculations, whereas the TURBOMOLE program [44,45] was employed for bare cluster calculations.

The computations were carried out using an IBM SP2 computer at KU Computing Center and DEC Alphastation 250 workstation at the Laboratory for Computational and Applied Chemistry at Kasetsart University, and clusters of IBM RISC/6000 workstation at Henry Eyring Center for theoretical Chemistry, University of Utah.

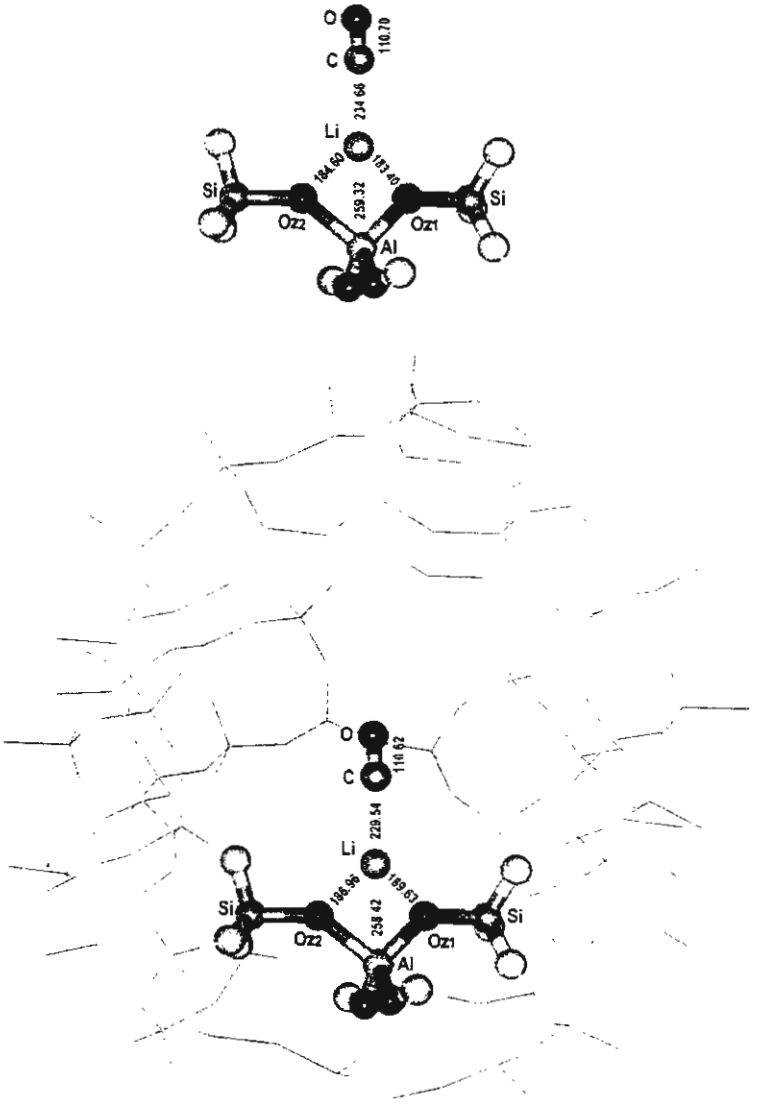

Fig. 4. Cluster and embedded cluster models of the Li-FAU/CO complex. Bond distances given in the figures are in pm.

3. Results and discussion

3.1. H-Faujasite (H-FAU) and metal-exchanged FAU (Li-FAU)

3.1.1. H-Faujasite (H-FAU)

Cluster and embedded cluster models for H-FAU zeolites are shown in Fig. 1. Selected optimized geometrical structures for bare quantum cluster and embedded cluster models employed to represent the Brønsted and cationic sites are evaluated at HF level of theory using the 6-31G(d,p) basis set, and are documented in Table 1.

Comparing the result between cluster and embedded cluster models, the Madelung potential has the effect of lengthening the O1–Hb bond distance (Brønsted acid site), and hence enhances the acidity of the Brønsted acid site. Our embedded cluster

Table 1
HF/6-31G (d,p) optimized geometrical parameters of the H-FAU and H-FAU/CO systems. (bond lengths are in pm and bond angles in degrees)

	H-FAU		H-FAU/CO	
	Bare cluster	Embedded	Bare cluster	Embedded
Al–H	238.27	236.26	240.96	237.99
O–H	95.11	95.32	95.45	95.84
Al–O1	174.61	172.94	174.88	173.14
Al–O2(H)	202.41	197.00	201.47	195.94
O1–Al–O2	88.93	93.09	89.51	93.64
Si–O2(H)	170.54	173.88	170.21	173.31
Si–O1	162.70	162.78	162.53	162.55
Si–O(H)–Al	139.71	141.08	139.67	141.01
C–O	–	–	111.07	110.98
H–C	–	–	227.69	223.45
q(H)	0.413838	0.422580	0.436389	0.445540
q(O1)	− 0.954577	− 0.940278	− 0.961167	− 0.942895
q(O2)	− 0.833108	− 0.852211	− 0.864249	− 0.887602

structures obtained are similar to those obtained from Greatbanks et al. employing a different embedded cluster approach via potential derived charges (PDC) [38]. Our predicted important bond lengths (O–H = 95.3, Si–O(H) = 173.9, Al–O1 = 172.9, Al–O2(H) = 197.0 pm) are virtually the same as reported by Greatbanks et al. (O–H = 95.4, Si–O(H) = 169.7, Al–O1 = 173.2, and Al–O(H) = 196.6 pm).

3.1.2. Metal-exchanged FAU (Li-FAU)

For the Li-FAU zeolite (see Fig. 2), the alkali-metal cation does not bind with a particular bridging oxygen atom in the $[AlO_4]^-$, but is symmetrically bidentated to O1 and O2 of $[AlO_4]^-$ tetrahedron. The symmetric binding between the alkali-metal and $[AlO_4]^-$ has been confirmed by an ESR experiment [47]. The interaction of the cationic metal with zeolite framework leads to substantial perturbation of the active acidic

Table 2
HF/6-31G (d,p) optimized geometrical parameters of the Li-FAU and Li-FAU/CO systems. (bond lengths are in pm, and bond angles in degrees)

	Li-FAU		Li-FAU/CO	
	Bare cluster	Embedded	Bare cluster	Embedded
Al–Li	257.99	258.11	259.32	258.42
Li–O1	182.13	187.93	183.40	189.63
Li–O2	183.14	186.46	184.60	186.96
O1–Li–O2	91.89	89.78	91.01	89.21
Al–O1	185.15	182.98	184.71	182.39
Al–O2	185.92	181.77	185.46	181.40
O1–Al–O2	90.05	92.84	90.33	93.26
Si–O2	164.56	166.58	164.30	166.14
Si–O1	164.35	164.85	164.09	164.54
Si–O2–Al	137.39	139.35	137.61	140.03
C–O	–	–	110.70	110.62
Li–C	–	–	234.66	229.54
q(Li)	0.641231	0.670350	0.492733	0.501856
q(O1)	− 1.037929	− 1.035260	− 1.037710	− 1.033770
q(O2)	− 1.032930	− 1.040422	− 1.032320	− 1.039655

Table 3
Calculated adsorption energies (kcal/mol) of CO on naked Li(I), bare quantum cluster and embedded cluster model of H-FAU and Li-FAU zeolites

	Naked	Embedded		3T Quantum cluster		Embedded		3T Quantum cluster	
	Li/CO	Li-ZSM-5/CO	Li-FAU/CO	Li-ZSM-5/CO	Li-FAU/CO	H-ZSM-5/CO	H-FAU/CO	H-ZSM-5/CO	H-FAU/CO
ΔE	−14.62	−10.78	−9.14	−8.04	−8.05	−6.09	−4.34	−3.61	−3.18
ΔE (BSSE)	−13.14	−8.56	−6.69	−5.77	−5.81	−4.95	−3.20	−2.25	−1.90

site. In particular, comparing the embedded cluster results listed in Table 2 for H-FAU and Li-FAU systems, we found the Al–O2(H) distance is shortened by 15.2 pm, while the other Al–O1 distance is elongated by 10.0 pm; similarly the Si–O2 (H) bond shortened by 7.3 pm, while the Si–O1 bond elongated by 2.1 pm; but the O1–Al–O2 angle has no significant change upon metal exchange. In a reciprocal effect, the zeolite framework reduces the Li cation charge to 0.67 a.u. The Madelung potential was found to have a large effect on the structure of Li-ZSM-5 zeolite. The oxygen atoms surrounding the cation in the bare quantum cluster and the environmental crystal in the embedded cluster via SCREEP can reduce the cationic strength, as depicted in Fig. 2. The extent of alkali···Oz distances increase with embedded model ($Li\cdots O_{1z} = 182.1$ pm vs. 187.9 pm and $Li\cdots O_{2z} = 183.1$ pm vs. 186.5 pm), indicating a weakening of the attachment of the metal cation to the zeolite framework. One can expect that, in this case, adsorption on the Li-FAU will be affected by the presence of the Madelung field.

3.2. The interaction of H-aluminosilicate (H-FAU) and Li-exchanged Faujasite (Li-FAU) with carbon monoxide

3.2.1. The interaction of H-zeolite (H-FAU) with carbon monoxide

Cluster and embedded cluster models for the adsorption of CO on H-FAU and Li-FAU zeolite are illustrated in Figs. 3 and 4, respectively. Selected geometrical parameters of the adduct complexes are listed in Tables 1 and 2. Adsorption energies evaluated by employing different models are given in Table 3.

The changes in the structural parameters of the CO and zeolite upon complexation are minute, but very impressive. The results are in accordance with Gutmann's rules [46], i.e. a lengthening of the O–H bond, shortening of the Si–O, Al–O and lengthening of Si–H bonds.

The intermolecular H···C distance of zeolite/CO adduct (within the ZO–H···CO bond) was calculated to be 227.7 pm via the cluster model. Including the Madelung potentials shortens this distance by 4.2 pm. This is also reflected in the calculated adsorption energies (Table 3), which increase by 1.30 kcal/mol upon Madelung potentials inclusion.

The interaction energy obtained from the embedded cluster is calculated to be −3.20 kcal/mol, which may be compared with the experimental range of 3.25–4.10 kcal/mol obtained by Gupta et al. [48] for an acidic zeolite of H–X using a range of acid site compositions. Agreement between the theory and the experiment is satisfactory, especially for the embedded cluster model.

3.2.2. The interaction of alkali-metal-exchanged aluminosilicates (Li-FAU) with carbon monoxide

In order to investigate the cationic effect on the interaction of sorbates in the alkali-metal zeolite/[CO], the naked alkali-metal ions/[CO] adducts have also been performed and compared with the cluster and embedded results.

The optimized geometries for the quantum cluster Li-FAU/CO and the embedded complexes are presented in Table 2. The binding of the naked Li(I) ion to the carbon monoxide leads to changes in geometrical structure parameters which are larger than those obtained for the Li-FAU/CO and the embedded complexes. The optimized Li···CO distances are found to be 226.9 pm for the simple naked Li(I)/CO, 229.5 pm for the embedded cluster, and 234.7 pm for the quantum cluster, the corresponding energies are −14.62(−13.14), −9.14(−6.69), and −8.05(−5.81) kcal/mol, respectively, values in parenthesis are BSSE corrected. Taking into account the BSSE does not change the trend. One can see that the adsorption energy of the embedded cluster model lies between those of the bare quantum cluster model and the simple naked Li/CO system. All quantities were overestimated because the electrostatic field generated by the simple naked cation is too large compared to the bare quantum cluster model, where it is reduced by the surrounding oxygen atoms. The embedded results are found to improve on the bare quantum cluster results in the calculation of interaction energies. The interaction energy of −6.69 kcal/mol for the embedded cluster model Li-FAU/CO that compares well with the adsorption energy of −6.7 kcal/mol for Na-exchanged Y zeolites complex [49].

Another point of interest is the comparison of the results obtained using both cluster and embedded

cluster models for exploring the different types of zeolites. The effects of the Madelung potential are more profound in the adsorption energies of CO on both Li-ZSM-5 and Li-FAU zeolites, as listed in Table 3.

For cluster model, Li-ZSM-5/CO and Li-FAU/CO complexes have virtually the same binding energies (Table 3). We found that the Madelung potential increases the binding energy by 2.74 kcal/mol in the Li-ZSM-5 and by about 1 kcal/mol in the Li-FAU zeolites. With the inclusion of basis-set-superposition-error correction and the effects of Madelung potential, we predict that the Li-ZSM-5/CO complex is more stable by about 1.9 kcal/mol as compared to the Li-FAU/CO complex. Thus, the Madelung potential was found to reveal that acidity of zeolite does not depend only on the acidic site center, but also on the framework structure where the acidic site is embedded.

4. Conclusions

The adsorption of carbon monoxide on H-Faujasite (H-FAU) and metal-exchanged Li-FAU zeolites has been investigated by means of both the quantum cluster and the embedded ab initio cluster approaches. For the H-FAU/CO complexes, the adsorption energy of the bare quantum cluster is evaluated to be −1.90 kcal/mol. Inclusion of the Madelung potential, via the Surface Charge Representation of the Electrostatic Embedding Potential (SCREEP) method, has a pronounced influence on the OH distance, hence increasing the binding energies of H-FAU/CO (−3.20 kcal/mol). The results obtained are in agreement with experimental data. For adsorption of CO on the metal-exchanged zeolites, the binding energies of the complexes obtained from the effect of Madelung potential can be employed to investigate the different types of zeolites. For the bare quantum clusters, Li-ZSM-5/CO and Li-FAU/CO complexes, have almost the same binding energies (−5.77 vs. −5.81 kcal/mol) while the binding energies derived from the embedded method of Li-ZSM-5/CO are calculated to be −8.56 kcal/mol which are larger than those obtained from the Li-FAU complex (−6.69 kcal/mol), indicating that the ZSM-5 is more acidic than that of FAU zeolites and leads to a better agreement with experimental observation. The results obtained in the present study suggest that the embedded cluster approach yield a more accurate and practical model than the bare quantum cluster for exploring zeolite framework and catalytic properties.

Acknowledgements

This work was supported by donors of the Thailand Research Fund (TRF) in supporting the research career development project (The TRF Research Scholar) and Royal Golden Jubilee PhD Program, as well as the Kasetsart University Research and Development Institute (KURDI) to J.L. Our sincere thanks are due to Professor R. Ahlrichs (Karlsruhe, Germany) and Professor T.N. Troung (University of Utah, Salt Lake City, USA) for their continued support of this work.

References

[1] J. Klinowski, Chem. Rev. 91 (1991) 1459.
[2] J.M. Thomas, Sci. Am. 266 (1992) 82.
[3] G.J. Kramer, R.A. van Santen, C.A. Emeris, A.K. Nowak, Nature 363 (1993) 529.
[4] E. Kassab, J. Fouquet, M. Allavena, E.M. Evleth. J. Phys. Chem. 97 (1993) 9034.
[5] C.T.W. Chu, C.D. Chang, J. Phys. Chem. 89 (1985) 1569.
[6] M.A. Makarova, S.P. Bates, J. Dwyer, J. Am. Chem. Soc. 117 (1995) 11309.
[7] J. Das, C.V.V. Satyanaryana, D.K. Chakrabarty, S.N. Piramanayagam, S.N. Shringi, J. Chem. Soc. Faraday Trans. 88 (1992) 3255.
[8] S.R. Blaszlowski, R.A. van Santen, J. Phys. Chem. 99 (1995) 11728.
[9] H.J. Soscun, P.J. Omalley, A. Hinchliffe, J. Mol. Struct. (Theochem) 341 (1995) 237.
[10] J. Limtrakul, S. Pollman-Hannongbua, J. Mol. Struct. (Theochem) 280 (1993) 139.
[11] J. Limtrakul, J. Mol. Struct. 288 (1993) 105.
[12] J. Limtrakul, Chem. Phys. 193 (1995) 79.
[13] J. Limtrakul, P. Treesukol, M. Probst, Chem. Phys. 215 (1997) 77.
[14] J. Limtrakul, U. Onthong, J. Mol. Struct. 435 (1997) 181.
[15] J. Limtrakul, D. Tantanak, J. Mol. Struct. 358 (1995) 179.
[16] J. Limtrakul, D. Tantanak, Chem. Phys. 208 (1996) 331.
[17] J.A. Zygmunt, L.A. Curtiss, L.E. Iton, M.K. Erhardt, J. Phys. Chem. 100 (1996) 6663.
[18] M. Krossner, J. Sauer, J. Phys. Chem. 100 (1996) 6199.
[19] F. Haase, J. Sauer, J. Am. Chem. Soc. 117 (1995) 3780.
[20] A.T. Bell, Catalysis Today 38 (1997) 151.

[21] M. Katoh, T. Yamazaki, H. Kamijo, S. Ozawa, Zeolites 15 (1995) 591.
[22] H.V. Brand, A. Redondo, P.J. Hay, J. Phys. Chem. B 101 (1997) 7691.
[23] I.N. Senchenya, E. Garrone, P. Ugliengo, J. Mol. Struct. (Theochem) 368 (1996) 93.
[24] J. Sauer, P. Ugliengo, E. Garrone, V.R. Saunders, Chem. Rev. 94 (1994) 2095.
[25] P. Geerling, N. Tariel, A. Botrel, R. Lissillour, W.J. Morlier, J. Phys. Chem. 88 (1984) 5752.
[26] P. Ugliengo, V.R. Saunders, E. Garrone, J. Phys. Chem. 93 (1989) 5210.
[27] S. Bates, J. Dwyer, J. Phys. Chem. 97 (1993) 5897.
[28] K.M. Neyman, P. Strodel, S.Ph. Ruzankin, N. Schlensog, H. Knozinger, N. Rosch, Catal. Lett. 31 (1995) 273.
[29] S. Ikuta, Chem. Phys. 95 (1985) 235.
[30] S. Ikuta, Chem. Phys. 109 (1984) 550.
[31] A.M. Ferrari, P. Ugliengo, E. Garrone, J. Chem. Phys. 105 (1996) 4129.
[32] N.U. Zhanpeisov, H. Nakatsuji, M. Hada, H. Nakai, M. Anpo, Catl. Lett. 42 (1996) 173.
[33] K.C. Hass, W.F. Schneider, J. Phys. Chem. 100 (1996) 9292.
[34] W.F. Schneider, K.C. Hass, R. Ramprasad, J.B. Adams, J. Phys. Chem. 100 (1996) 6032.
[35] B.L. Trout, A.K. Chakraborty, A.T. Bell, J. Phys. Chem. 100 (1996) 4173.
[36] D.A. Dixon, J.L. Gole, A. Komornicki, J. Phys. Chem. 92 (1988) 1378.
[37] E.V. Stefanovich, T.N. Troung, J. Phys. Chem. B 102 (1998) 3018.
[38] S.P. Greatbanks, I.H. Hillier, N.A. Burton, P. Sherwood, J. Chem. Phys. 105 (1996) 3370.
[39] R. Dovesi, V.R. Saunders, C. Roetti, CRYSTAL 92. An ab initio Hartree–Fock LCAO Program for Periodic Systems, Theoretical Chemistry Group, University of Torino and SERC, Daresbury Laboratory, 1992.
[40] L. Campana, A. Selloni, J. Weber, A. Pasquarello, I. Papai, A. Goursot, Chem. Phys. Lett. 226 (1994) 245.
[41] E.H. Teunissen, C. Roetti, C. Pisani, A.J.M. de Man, A.P.J. Jansen, R. Orlando, R.A. van Santen, R. Dovesi, Modelling Simul. Matter. Sci. Engng 2 (1994) 921.
[42] W.J. Mortier, E. van der Bosche, J.B. Uytherhoven, Zeolites 4 (1984) 41.
[43] M.J. Frisch, G.W. Trucks, H.B. Schlegel, P.M.W. Gill, B.G. Johnson, M.W. Wong, J.B. Foresman, M.A. Robb, M. Head-Gordon, E.S. Replogle, R. Gomperts, J.L. Andres, K. Raghavachari, I.S. Binkley, C. Gonzalez, R.L. Martin, D.J. Fox, D.J. DeFrees, J. Baker, J.J.P. Stewart, J.A. Pople, GAUSSIAN, Guassian Inc., Pittsburgh, 1994.
[44] R. Ahlrichs, M. Baer, M. Haeser, H. Horn, C. Koemel, Chem. Phys. Lett. 162 (1989) 165.
[45] M. Haeser, R. Ahlrichs, J. Comput. Chem. 10 (1989) 104.
[46] V. Gutmann, The Donor–Acceptor Approach to Molecular Interaction, Plenum, New York, 1978.
[47] H. Hosono, H. Kawazoe, J. Nishii, J. Kanazawa, J. Non Cryst. Solid 51 (1982) 217.
[48] N.M. Gupta, V.S. Kamble, A.K. Roa, R.M. Iyer, J. Catal. 120 (1989) 432.
[49] V. Bolis, B. Fubini, E. Garrone, E. Giamello, C. Morterra, in: C. Morterra, A. Zecchina, G. Costa (Eds.), Structure and Reactivity of Surfaces, Elsevier, Amsterdam, 1989.

V.

Adsorption/Reaction in Zeolites

Reactions and mechanisms of molecular probes on Faujasite

- Journal of Molecular Structure, 2001, 560, 167-177.
- Stud. Surf. Sci. Catal., 2001, 135, 2469-2476.

ELSEVIER

Journal of Molecular Structure 560 (2001) 169–177

Journal of
MOLECULAR
STRUCTURE

www.elsevier.nl/locate/molstruc

Effect of high coverages on proton transfer in the zeolite/water system

J. Limtrakul*, P. Chuichay, S. Nokbin

Department of Chemistry, Laboratory for Computational and Applied Chemistry, Faculty of Science, Kasetsart University, Bangkok 10900, Thailand

Received 8 June 2000; revised 21 August 2000; accepted 8 September 2000

Abstract

The density functional theory and Hartree–Fock methods were used to investigate the proton transfer reaction for a series of model clusters of zeolite/$(H_2O)_n$; $n = 1, 2, 3$, and 4. Without promoted water, the hydrogen-bonded dimer of the water/zeolite system exists as a simple hydrogen-bonded complex, $ZOH.(H_2O)_2$, and no proton transfer occurs from zeolite to water. The third promoted water, $ZOH(H_2O)_2H_2O$, was found to induce a pathway for proton transfer, but at least addition two promoted molecules, $ZO(H_3O^-)H_2O(H_2O)_2$, must be involved for complete proton transfer from zeolite to H_2O. The results show that the hydronium ion in water cluster adsorbed on zeolite, $ZO(H_3O^+)(H_2O)_3$, can considerably affect the structure and bonding of the hydrogen-bonded dimer of water. The O···O distance is contracted from 2.818 Å found in the neutral complex, $ZOH(H_2O)_4$, to 2.777 Å for ion-pair complex, $ZO(H_3O^+)(H_2O)_3$. The distance between the oxygen of the hydronium ion and the zeolitic acid site oxygen is predicted to be 2.480 Å which is in good agreement with the experimentally observed value of 2.510 Å. The corresponding density functional adsorption energy of the high coverages of adsorbing molecules on zeolite is calculated to be −9.14 kcal/mol per molecule at B3LYP/6-311+G(d,p) level of theory and compares well with the experimental observation of −8.20 kcal/mol.

Keywords: Zeolite/water system; Hartree–Fock method; Proton transfer

1. Introduction

The acidity of zeolitic catalysts generated from the surface hydroxyls (≡Si–OH–Al≡) is responsible for catalytic function and have led to numerous important industrial applications, such as catalysts and adsorbents which have been employed for petrochemical processes and for the production of fine chemicals [1–14]. Of particular interest in this active research is the adsorption structure of methanol and water and the question of whether these probe molecules are protonated or not at acid zeolite catalysts are discussed in depth [15–25]. In spite of a large volume of documents about zeolite research, the details of structures and reaction mechanisms of adsorption and particularly of protonation/deprotonation are still incomplete and, mainly, to be solved. These understandings are the basis for catalytic reaction mechanisms and hence enhance the rational design of improved catalysts.

In this work, the interaction of water clusters with generic zeolites (H-ZOH) and Faujasite (FAU) are investigated for the first time by the density functional theory (DFT), and HF with the aims of: (a) investigating the important consequences of adsorbed probe

* Corresponding author. Tel.: +66-2-942-8900; fax: +66-2-579-3955.

E-mail address: fscijrl@ku.ac.th (J. Limtrakul).

0022-2860/01/$ - see front matter
PII: S0022-2860(00)00737-7

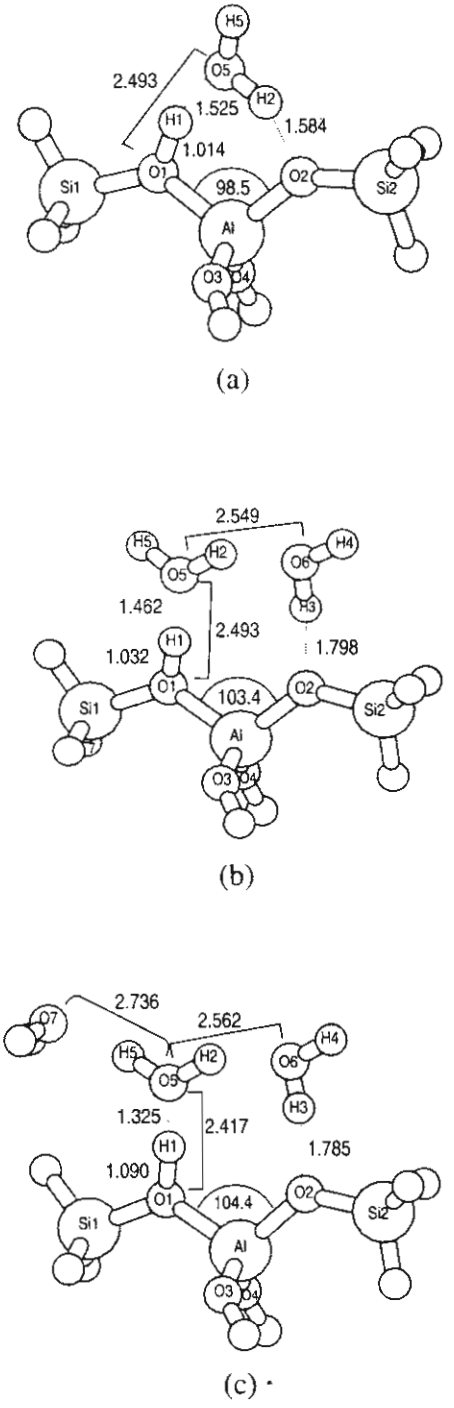

Fig. 1. The fully optimized geometrical structures for generic zeolites. $[H_3SiOHAl(OH)_2OSiH_3][H_2O]_n$ were investigated at B3LYP/6-31G(d,p) levels of theory.

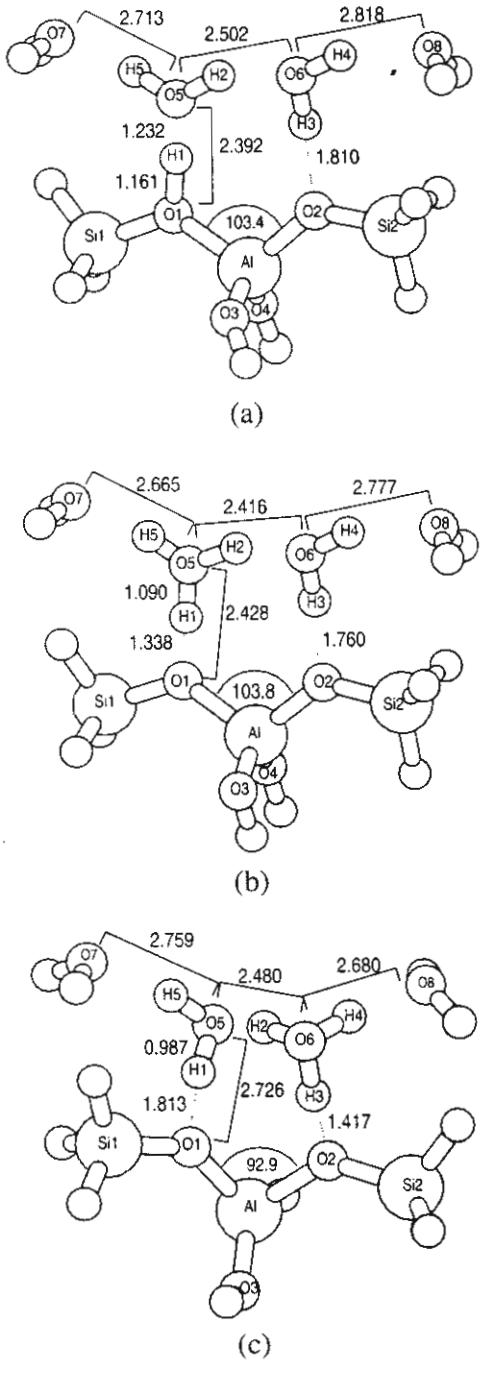

Fig. 2. The fully optimized geometrical structures of zeolite/$(H_2O)_3$: (a) neutral complex of generic zeolite/$(H_2O)_4$ system; (b) ion-pair complex on generic zeolite/$(H_2O)_4$ system; (c) ion-pair structure of water adsorption on faujasite zeolite/$(H_2O)_4$ system.

Table 1
Adsorption energies of water clusters on zeolites (kcal/mol)

Models	B3LYP/6-31G(d.p)			
	Generic zeolite		Faujasite zeolite	
	Neutral[a]	Ion-pair[a]	Neutral[a]	Ion-pair[a]
Zeolite /H_2O	−18.25 (−13.93)	–	−20.92 (−15.99)	–
Zeolite /$(H_2O)_2$	−29.69 (−21.93)	–	−33.84 (−23.43)	–
Zeolite /$(H_2O)_3$	−40.36 (−28.50)	–	−35.85 (−29.56)	–
Zeolite /$(H_2O)_4$	−50.30 (−33.67)	−50.65 (−32.45)	–	−55.96 (−36.56)

[a] Values in parenthesis are obtained at B3LYP/6-311+G(d,p)//6-31G(d,p) level of theory.

molecules at low and high coverages, i.e. $(H_2O)_n$, where n denotes the amount of water molecule coverages; (b) obtaining structures and the reaction mechanism of high coverages in zeolite catalyst.

2. Method

We employed the adsorption clusters illustrated in Figs. 1 and 2 as the models of water molecules adsorption on zeolites $[H_3SiOHAl(OH)_2OSiH_3]/[H_2O]n$,; n = 1–4 and their possible ion-pair species. The cluster is selected to model specially to Faujasite zeolite with the symmetry C_1. In models employed the dangling bonds of "surface" oxygen atoms are terminated by H atoms and the Si–H bonds are aligned with the corresponding Si–O bonds of the structure of faujasite zeolite [26].

Full geometry optimization of the cluster models mentioned above was carried out with the DFT methods employing B3LYP density functional. This functional has been recently demonstrated by us to yield accurate results about molecular structures, and vibrational frequencies for zeolites [27–32]. Additionally, calculations with the 6-311+G(d,p) basis set were performed for some models. The DFT performs perfectly well at this level of theory, which is in good agreement with the CPF and G1 results [27,28]. All density functional computations were performed using the program GAUSSIAN-94 [33].

For the HF calculations, we employed the TURBOMOL code [34,35] which is based on the direct SCF method of Almloęf et al. [36]. Geometry optimization was terminated when the gradients norm with respect to internal coordinates was less than 10^{-3} E_h/a_0. The energy change was then below 5×10^{-6} a.u.

The cluster computations were carried out using DEC Alphastation 250 and HP 9000/700 workstations at the Laboratory for Computational and Applied Chemistry at Kasetsart University.

3. Results and discussion

The fully optimized geometrical structures constrained at C_s symmetry for generic zeolite, $[H_3SiOHAl(OH)_2OSiH_3][H_2O]_n$ and at C_1 symmetry for specific type Faujasite/$[H_2O]_n$ (see Figs. 1 and 2) are investigated at HF and B3LYP levels of theory using 6-31G** basis set. The adsorption energies and selected parameters for two theoretical approaches are summarized in Tables 1–6. Complete coordinates and other calculation details are available by E-mail: fscijrl@ku.ac.th.

Comparing the HF structure of $H_3SiOHAl(OH)_2OSiH_3$ with the B3LYP structure, it is seen that the Si–O(H), Al–O(H), O–H bonds of the former are shorter than the latter. Note that the HF results always yield an OH bond which is too short as compared to the experimental result [37].

Further support for the reliability of using this model is confirmed by the results of NMR measurement [38]: the Al···H of H-Faujasite has been estimated to be 2.380 ± 0.004 Å, whereas our computed distance at B3LYP and HF levels of theory are 2.397 and 2.416 Å. respectively.

3.1. One and two water molecules per acid site

Two representative cluster models of water adsorption on zeolites are investigated. In one of these, the hydrogen-bonded structures are stabilized on the

Table 2
Comparison of H_2O adsorption on H-Zeolite with previously published theoretical and experimental results

Method	Cluster size	Cluster termination	Cluster constrains	No. of water	Basis set	ΔE (kcal/mol)	Ref.
DFT/B3LYP	3T	H	Edge (Fau)	1	6-31G(d, p)	−20.92	This work
DFT/B3LYP	3T	H	Edge (Fau)	2	6-31G(d, p)	−16.92	This work
DFT/B3LYP	3T	H	Edge (Fau)	1	6-31G(d, p)// 6-311+G(d, p)	−15.99	This work
DFT/B3LYP	3T	H	Edge (Fau)	2	6-31G(d, p)// 6-311+G(d, p)	−11.72	This work
DFT/B3LYP	5T	H	Edge (Fau)	1	6-31G(d)	−20.50	[28]
DFT/B3LYP	5T	OH	Edge (ZSM-5)	1	6-31G(d, p)	−19.70	[45]
DFT/B3LYP	5T	OH	Edge (ZSM-5)	2	6-31G(d, p)	−11.80	[45]
MP2	5T	H	None	1	DZP(H,S,Al);TZP(O)	−18.90	[41]
DFT/BP	5T	H	None	1	DZP(H,S,Al);TZP(O)	−17.94	[41]
DFT/BP	5T	H	None	2	DZP(H,S,Al);TZP(O)	−14.28	[41]
MP2	3T	OH	None	1	6-31++G(d)	−22.08	[43]
DFT/BLYP	3T	OH	None	2	DZVP2	−16.00	[44]
DFT/BLYP	4T	OH	None	1	DZVP2	−12.97	[44]
experiment				1		−12.10	[15]
experiment				2		−8.10	[15]

Table 3
Structure parameters of Zeolite/H_2O system

Bond (Å) and angle (°)	Generic zeolite/H_2O		Faujasite zeolite/H_2O	
	HF/3-21G Neutral	B3LYP/6-31G(d, p) Neutral	HF/3-21G Neutral	B3LYP/6-31(d, p) Neutral
Al–O1	1.826	1.904	1.864	1.952
Al–O2	1.756	1.776	1.779	1.796
Al–O3	1.693	1.731	1.736	1.740
Al–O4	1.693	1.731	1.718	1.724
⟨Al–O⟩	1.742	1.785	1.774	1.803
O1–O5	2.400	2.493	2.424	2.523
O1–H1	1.038	1.014	1.055	1.033
O5–H1	1.416	1.525	1.387	1.503
O5–H5	0.958	0.960	0.963	0.967
O5–H2	1.001	0.984	1.022	0.996
O1–H1–O5	155.7	157.8	166.8	168.5
O2–Al–O1	102.4	98.5	92.5	89.9

Brønsted site. The other is a type of protonated model, in which hydronium ions forms two hydrogen bonds towards the unprotonated zeolite framework. All investigated cluster models yielded only one minimum as hydrogen-bonded physisprobed water complexes, regardless of whether the initial framework structure had H_2O or H_3O^+. Similar conclusions to our results have just recently been reported by Sauer et al., FT-IR [39,40] and ab initio [41] studies of water adsorption on zeolite support the direct clear evidence for the hydrogen-bonded adsorption of water.

The changes in the structural parameters of the zeolite upon complexation with water are minute but impressive. The results are in accordance with Gutmann's rules [42], i.e. a lengthening of the bridging O–H bond, a shortening of Al–O adjacent to this bond and a lengthening of Al–O (not adjacent to it).

Table 4
Structure parameters of Zeolite/$(H_2O)_2$ system

Bond (Å) and angle (°)	Generic Zeolite/$(H_2O)_2$		Faujasite Zeolite/$(H_2O)_2$	
	HF/3-21G Neutral	B3LYP/6-31G(d, p) Neutral	HF/3-21G Neutral	B3LYP/6-31G(d, p) Neutral
Al–O1	1.814	1.888	1.849	1.941
Al–O2	1.755	1.780	1.767	1.793
Al–O3	1.698	1.734	1.738	1.746
Al–O4	1.698	1.734	1.720	1.726
⟨Al–O⟩	1.741	1.784	1.768	1.801
O1–O5	2.420	2.493	2.443	2.521
O1–H1	1.063	1.032	1.057	1.043
O5–H1	1.358	1.462	1.403	1.484
O5–H5	0.978	0.973	1.008	0.998
O5–H2	0.978	0.973	0.963	0.967
O5–O6	2.433	2.549	2.465	2.634
O6–H3	0.996	0.983	1.000	0.986
O6–H4	0.960	0.961	0.962	0.965
O1–H1–O5	177.0	177.3	166.5	171.9
O2–Al–O1	108.2	103.7	93.1	90.2
O5–H2–O6	146.5	148.0	152.5	158.8

Table 5
Structure parameters of Zeolite/$(H_2O)_3$ system

Bond (Å) and angle (°)	Generic zeolite/$(H_2O)_3$		Faujasite zeolite/$(H_2O)_3$	
	HF/3-21G Ion-pair	B3LYP/6-31G(p. d) Neutral	HF/3-21G Ion-pair	B3LYP/6-31G(d. p) Neutral
Al–O1	1.792	1.873	1.796	1.937
Al–O2	1.764	1.783	1.785	1.794
Al–O3	1.705	1.737	1.745	1.748
Al–O4	1.705	1.737	1.730	1.736
⟨Al–O⟩	1.741	1.783	1.764	1.804
O1–O5	2.379	2.417	2.401	2.468
O1–H1	1.239	1.090	1.304	1.090
O5–H1	1.141	1.325	1.103	1.381
O5–H5	0.996	0.981	0.986	0.982
O5–H2	0.996	0.981	1.036	0.993
O5–O6	2.411	2.562	2.397	2.653
O6–H3	1.004	0.984	0.962	0.987
O6–H4	0.960	0.961	1.020	0.966
O7–O5	2.602	2.736	2.580	2.790
O1–H1–O5	176.8	176.6	172.0	173.8
O2–Al–O1	109.4	104.4	65.7	90.4
O5–H5–O7	171.4	168.4	161.0	170.1
O5–H2–O6	151.4	148.2	151.5	160.7

Table 6
Structure parameters of Zeolite/$(H_2O)_4$ system

Bond (Å) and angle (°)	Generic zeolite/$(H_2O)_4$			Faujasite zeolite/$(H_2O)_4$	
	HF/3-21G Ion-pair	B3LYP/6-31G(d. p) Neutral	Ion-pair	HF/3-21G Ion-pair	B3LYP/6-31G(d, p) Ion-pair
Al–O1	1.789	1.863	1.830	1.756	1.864
Al–O2	1.762	1.785	1.800	1.808	1.809
Al–O3	1.707	1.739	1.742	1.729	1.396
Al–O4	1.707	1.739	1.742	1.743	1.755
⟨Al–O⟩	1.741	1.782	1.779	1.759	1.706
O1–O5	2.398	2.392	2.428	2.608	2.726
O1–H1	1.300	1.161	1.337	1.659	0.987
O5–H1	1.100	1.232	1.090	0.989	1.813
O5–H5	1.005	0.989	0.985	0.976	0.984
O5–H2	1.005	0.989	1.034	1.425	1.441
O5–O6	2.384	2.502	2.416	2.409	2.480
O6–H3	0.990	0.979	0.988	1.096	1.069
O6–H4	0.971	0.973	0.974	0.986	0.996
O7–O5	2.598	2.713	2.665	2.681	2.759
O6–O8	2.708	2.818	2.777	2.603	2.680
O1–H1–O5	176.8	177.1	179.8	159.2	152.3
O2–Al–O1	109.7	103.4	103.8	95.8	92.9
O5–H5–O7	171.2	169.6	168.8	156.5	166.9
O5–H2–O6	152.4	151.5	155.7	155.0	166.1
O6–H4–O8	156.4	157.6	156.4	171.7	172.2

Similar trends are also observed for two water molecules per acid site. The O–H distance in the optimized structure of zeolite/H_2O and zeolite/$(H_2O)_2$ adducts (Fig.1) are evaluated to be 1.014 and 1.032 Å, respectively. The lengthened O–H distance of the latter model refects an increase of the binding energy (see Table 1) (−13.93 versus −21.93 kcal/mol.). Comparison of H_2O adsorption on H-zeolite with previous quantum calculations [43–45] and experimental measurement [15] is also documented in Table 2. Our findings agree closely with those reported by Zygmunt et al. [43], Gale [44], and Rice et al. [45] on the basis of DFT calculations carried out with a 3T, 4T, or a 5T cluster, respectively. The calculated adsorption energies and those estimated from the experimental values are different for the case of one adsorbed H_2O molecule but not for the adsorption of a second H_2O molecule. Since the uncertainties in the experimental adsorption energy values are not known [45], it is difficult to discuss further.

Attempts have been made to observe the $Z^-/[H_3O]^+[H_2O]$, an initial structure in which a hydronium ion is optimized. The OH bond of H_3O^+ and the hydrogen bond angle (O–H...O) in the complex is constrained at the optimized H_3O^+ and 180° respectively. However, during the optimization, the proton of H_3O^+ is transferred to the zeolite, and the final equilibrium complex H–Z/$[H_2O][H_2O]$ is obtained. The present finding is consistent with those of Gale [44] and Rice et al. [45] that no evidence of proton transfer is observed with either one or two H_2O molecules adsorbed on the zeolitic cluster models. The experimentally observed reduction of adsorption energy per molecule when passing from one to two molecules per site of about 4.06 kcal/mol is reproduced by our predicted value of 4.27 kcal/mol. We note that differences in cluster size, method of cluster termination, the presence or absence of structural constraints may contribute to the observed differences on the geometry.

3.2. Three and four water molecules per acid site

The equilibrium structures for Zeolite/$(H_2O)_n$, n = 3 and 4, are illustrated in Figs. 1 and 2 together with the key parameters and corresponding adsorption energies. There are two types of these clusters: the hydrogen-bonded and ion-pair forms. From the clusters shown in Fig. 2 and geometrical parameters documented in Tables 5–6, the data derived indicates that the zeolitic proton remains non-transferred in the zeolite/$(H_2O)_n$ complexes until at least three, preferably four, water molecules are solvated around the Brønsted acid site.

The intermolecular O···O distances in the optimized structure of zeolite/$(H_2O)_n$ complexes (within the OH···O hydrogen bond) are evaluated to be 2.493, 2.417, and 2.392 Å for zeolite/$(H_2O)_2$, zeolite/$(H_2O)_3$ and zeolite/$(H_2O)_4$, respectively. The contracted O···O distances with higher coverage reflect an increase of the O–H Brønsted distance (1.032, 1.090 and 1.161 Å). It does nevertheless show at the low level of theory (HF/3-21G) that zeolite/$(H_2O)_3$ starts deprotonation when solvated by three water molecules. Note that this ion-pair structure is achieved only at HF/3-21G, while only hydrogen-bonded $ZH[H_2O][H_2O]_2$ is obtained at the B3LYP level of theory. This may be due in part to the over binding at this low theoretical level.

With the very high coverages, four water molecules, the protonation seems certain and the ion-pair structure is achieved only for the specific type Faujasite. Our results clearly show the important influence of water loading for the formation of protonated species on the zeolite. The bridging OH bond length of zeolite increases with each probe molecule successively added. The optimized structure parameters of $[H_3SiOAl(OH)_2SiH_3]^-/[H_3O]^-[H_2O]_3$ are illustrated in Fig. 2b and documented in Table 6. For this ion-pair structure, the $[H_3O]^+$ cation forms three very strong hydrogen bonds towards the neighboring water molecules and the negatively charged zeolite. The Al–O1, and Al–O2 distances are 1.864 and 1.809 Å, which are longer than found in anionic zeolite (both at 1.776 Å). For these high coverages, the hydronium ion is found to have a strong effect on the hydrogen-bonded dimer of water. The O(6)···O(8) distance of $[H_3SiOAl(OH)_2SiH_3]^-/[H3O]^+[H2O]_3$ is contracted by 0.04 Å as compared to the neutral hydrogen-bonded system, $[H_3SiOAl(OH)_2SiH_3]/[H_2O][H_2O]_3$ for generic zeolite (Fig. 2b and c). The energy for conversion of $[H_3SiOAl(OH)_2SiH_3]^-/[H_3O]^+[H_2O]_3$ to the neutral hydrogen-bonded complex $[H_3SiOAl(OH)_2SiH_3]/[H_2O][H_2O]_3$ is 0.34 kcal/mol.

The most stable structure of water adsorption on Faujasite zeolite is illustrated in Fig. 2c. It should be noted that there are much deviations between the

isolated H_3O^+ structure and those for H_3O^+ in the zeolite/water complex. This observation is due mainly to the fact that the hydronium ion is stabilized by interacting with solvating water molecules and the anionic zeolite framework. The acid hydrogen sits 1.417 Å from the zeolitic framework oxygen, O(2) and 1.069 Å from the oxygen of the H_3O^+ ion. The oxygen of the hydronium ion is located at 2.480 Å from the acid site oxygen O(2). This calculated $H_3O^+\cdots Oz$ distance can be compared well with the experimental observation of 2.51 Å for a weaker acid catalyst, silicoaluminosilicate (SAPO)[46]. The ion-pair complex, $[H_3SiOAl(OH)_2SiH_3]^-$ /$[H_3O]^+[H_2O]$ was somewhat similar to those of $HCl(H_2O)_4$ and $HBr(H_2O)_4$ [47] and other acid–water clusters previously investigated, and was shown to indeed induce protonation of a variety of acids [48].

4. Conclusions

The influence of high coverages of adsorbing molecules on zeolites has been investigated by means of both density functional theory and Hartree–Fock methods. Equilibrium structures determined for the adsorbing molecules successively added from one to four molecules per acid site. While $[H_3SiOAl(OH)_2SiH_3]/[H_2O]$ and $[H_3SiOAl(OH)_2SiH_3]/[H_2O]_2$ are a hydrogen-bonded complex, cluster of $[H_3SiOAl(OH)_2SiH_3]/[H_2O]_4$ contains both types of ion-pair and neutral complexes. The ion-pair complex results from a prompt and complete proton transfer from zeolite to adsorbate that takes place in the high coverages. For the hydronium ion which is stabilized by additional adsorbing molecules, the distance between the oxygen of the hydronium ion and the zeolitic acid site oxygen is calculated to be 2.480 Å. This finding is in good agreement with the experimental observation of 2.510 Å for a weak zeolite acid catalyst, HSAPO-34. The corresponding adsorption energy of this complex is predicted to be −9.14 kcal/mol per molecule at B3LYP/6-311+G(d, p) level of theory and compares well with the measured adsorption heat of −8.20 kcal/mol in HZSM-5.

Acknowledgements

This work was supported by grants from the Thailand Research Fund (TRF) for supporting the research career development project (The TRF-scholar) and the Kasetsart University Research and Development Institute (KURDI). Our sincere thanks are due to Prof R. Ahlrichs (Karlsruhe, Germany) for his continued support of this work.

References

[1] J. Klinowski, Chem. Rev. 91 (1991) 1459.
[2] J.M. Thomas, Sci. Am. 266 (1992) 82.
[3] G.J. Kramer, R.A. Van Santen, C.A. Emeis, A.K. Nowak, Nature 363 (1993) 529.
[4] E. Kassab, J. Fouquet, M. Allavena, E.M. Evleth, J. Phys. Chem. 97 (1993) 9034.
[5] C.T.W. Chu, C.D. Chang, J. Phys. Chem. 89 (1985) 1569.
[6] K.J. Chao, L.J. Len, in: H.G. Karge, J. Weitkam (Eds.), Zeolites As Catalysts, Sorbents And Detergent Build. Elsevier, Amsterdam, 1989.
[7] J. Das, C.V.V. Satyanaryana, D.K. Chakrabarty, S.N. Piramanayagam, S.N. Shringi, J. Chem. Soc., Faraday Trans. 88 (1992) 3255.
[8] Y. Murakami, A. Iijima, J.W. Ward, New Developments in Zeolite Science and Technology, Kodancha, Tokyo, 1986.
[9] J. Limtrakul, S. Hannonbua, J. Mol. Struct. (Theochem) 280 (1993) 139.
[10] J. Limtrakul, J. Mol. Struct. (Theochem) 288 (1993) 105.
[11] J. Limtrakul, J. Yoinuan, J. Chem. Phys. 184 (1994) 51.
[12] J. Limtrakul, J. Yoinnan, D. Tantanak, J. Mol. Struct. (Theochem) 312 (1994) 183.
[13] J. Limtrakul, J. Yoinuan, D. Tantanak, J. Mol. Struct. 322 (1995) 151–159.
[14] J. Limtrakul, D. Tantannak, Chem. Phys. 208 (1996) 331.
[15] A. Ison, R.J. Gorte, J. Catal. 89 (1984) 150.
[16] G. Mirth, J.A. Lercher, M.W. Anderson, J. Klinnoski, J. Chem. Soc., Faraday Trans. 86 (1990) 3039.
[17] A. Jentys, G. Warecka, M. Derewinski, J.A. Lercher, J. Phys. Chem. 93 (1989) 4837.
[18] F. Haase, J. Sauer, J. Am. Chem. Soc. 117 (1995) 3780.
[19] S. Bates, J. Dwyer, J. Mol. Struct. (Theochem) 306 (1994) 57.
[20] A.G. Pelmenschikov, R.A. van Santen, J. Phys. Chem. 97 (1993) 10 678.
[21] L. Marchese, J. Chen, P.A. Wright, J.M. Thomas, J. Phys. Chem. 97 (1993) 8109.
[22] J. Limtrakul, Chem.Phys. 193 (1995) 79.
[23] S.P. Greatbanks, I.H. Hillier, N.A. Burton, J. Chem. Phys. 105 (1996) 3770.
[24] E. Nusterer, P.E. Bloechl, K. Schwarz, Angew. Chem. Int. Ed. 35 (1996) 175.
[25] A. Kogelbauer, A.A. Nikolopoulos, J.G. Goodwin Jr., G. Marcelin, J. Catal. 152 (1995) 122.
[26] W.J. mortier, E. van der Bosche, J.B. Uytherhoeven, Zeolites 4 (1984) 41.
[27] J. Limtrakul, D. Tantanak, J. Mol. Struct. (Theochem) 358 (1995) 179–193.

[28] J. Limtrakul, P. Treesukol, M. Probst, Chem. Phys. 215 (1997) 77–87.
[29] J. Limtrakul, U. Ongthong, J. Mol. Struct. 435 (1997) 181.
[30] J. Limtrakul, M. Kuno, P. Treesukol, J. Mol. Struct. 510 (1999) 131–147.
[31] J. Limtrakul, P. Khongpracha, S. Jungsuttivong, T.N. Troung, J. Mol. Catal. A 153 (2000) 155.
[32] J. Limtrakul, P. Khongpracha, S. Jungsuttivong, J. Mol. Strcut. 525 (2000) 155.
[33] M.J. Frish, G.W. Trucks, H.B. Schlegel, P.M.W. Gill, B.G. Johnson, M.W. Wong, J.B. Foresman, M.A. Robb, M. Head-Gordon, E.S. Replogle, R. Gomperts, J.L. Andres, K. Raghavachari, I.S. Binkley, C. Gonzalez, R.L. Martin, D.J. Fox, D.J. DeFrees, J. Baker, J.J.P. Stewart J.A. Pople, GAUSSIAN 94, Gaussian, Pittsburgh, 1994.
[34] R. Ahlrichs, R. Baer, M. Haeser, H. Horn, C. Koemel, Chem. Phys. Lett. 162 (1989) 165.
[35] M. Haeser, R. Ahlrichs, J. Comput. Chem. 10 (1989) 104.
[36] J. Almloef, K. Faegri Jr., K. Korsell, J. Comput. Chem. 3 (1982) 385.
[37] W.J. Hehre, L. Radom, P.A. Pople, P.v.R. Schleyer, Ab Initio Molecular Orbital Theory, Wiley, New York, 1987.
[38] D. Freude, J. Klinowski, H. Hamdan, Chem. Phys. Lett. 149 (1988) 355.
[39] F. Wakabayashi, J.N. Kondo, K. Domen, C. Hirose, J. Phys. Chem. 100 (1996) 1442.
[40] B. Lee, J.N. Kondo, K. Domen, F. Wakabayashi, J. Mol. Catal. A 137 (1999) 269.
[41] M. Krossner, J. Sauer, J. Phys. Chem. 100 (1996) 6199.
[42] V. Gutmann, The Donor–Acceptor Approach to Molecular Interactions, Plenum Press, New York, 1978.
[43] S.A. Zygmunt, L.A. Curtiss, L.E. Iton, M.K. Erhardt, J. Phys. Chem. 100 (1996) 6663.
[44] J.D. Gale, Top. Catal. 3 (1996) 169.
[45] M.J. Rice, A.K. Chakraborty, A.T. Bell, J. Phys. Chem. A 102 (1998) 7498.
[46] L. Smith, A.K. Cheetham, R.E. Morris, L. Marchese, J.M. Thomas, P.A. Wright, J. Chen, Science 271 (1996) 799–802.
[47] C. Conley, F.M. Tao, Chem. Phys. Lett. 301 (1999) 29–36.
[48] C. Lee, C. Sosa, M. Planas, J.J. Novoa, J. Chem. Phys. 104 (1996) 7081.

ELSEVIER Studies in Surface Science and Catalysis, 135 (2001) 2469-2476

High coverage effect on proton transfer of faujasite/water system: density functional embedded cluster approach

Jumras Limtrakul[a,*], Somkiat Nokbin[a], Parawan Chuichay[a], Pipat Khongpracha[a], Siriporn Jungsuttiwong[a], and Thanh N. Troung[b]

[a]*Laboratory for Computational & Applied Chemistry, Chemistry Department, Kasetsart University, Bangkok 10900, THAILAND; e-mail: fscijrl@ku.ac.th*

[b]*Henry Eyring Center for Theoretical Chemistry, Department of Chemistry, University of Utah, 315 S 1400 E, rm 2020, Salt Lake City, UT 84112, USA*

Quantum cluster and embedded cluster approaches were used to investigate the proton transfer reaction for a series of model clusters of zeolite/$(H_2O)_n$; n = 1, 2, 3, and 4, using the B3LYP/6-31G (d,p) level of theory. For both calculations, without promoted water, the hydrogen-bonded dimer of the zeolite/water system exists as a simple hydrogen-bonded complex, $ZOH(H_2O)_2$, and no proton transfer occurs from zeolite to water. The third promoted water, $ZOH(H_2O)_2H_2O$, was found to induce a pathway for proton transfer, but at least the addition of two promoted molecules, $ZO(H_3O^+)H_2O(H_2O)_2$, must be involved for complete proton transfer from zeolite to H_2O. Inclusion of the Madelung potential was found to increase the acidity of the Brønsted acid site, yielding the complete proton transfer from zeolite to H_2O in the presence of the third promoted water, $ZO(H_3O^+)(H_2O)_2$. The distance between the oxygen of the hydronium ion and the zeolitic acid site oxygen is predicted to be 2.512 Å for the embedded cluster which is in good agreement with the experiment.

1. INTRODUCTION

The acidity of zeolitic catalysts generated from the surface (≡Si-OH-Al≡) is responsible for the catalytic function and have led to numerous important industrial applications, such as catalysts and adsorbents which have been employed for petrochemical processes and for the production of fine chemicals. Of particular interest in this active research is the adsorption structure of methanol and water and the question of whether these probe molecules are protonated or not at acid zeolite catalysts are discussed in depth [1-12]. In spite of a large volume of documents about zeolite research, the details of structures and reaction mechanisms of adsorption, and particularly of protonation/deprotonation are still incomplete and, mainly, to be solved.

2. METHODS

Cluster and embedded cluster models were used to determine the structure of water molecules adsorption of zeolites $[H_3SiOHAl(OH)_2OSiH_3]/[H_2O]_n$; n = 1-4 and their possible ion-pair species. The cluster is selected to model specially to faujasite zeolite with the

symmetry C_1. In models employed, the dangling bonds of "surface" oxygen atoms are terminated by H atom and Si-H bonds are aligned with the corresponding Si-O bonds of the structure of faujasite zeolite [13].

In the embedded cluster model, the static Madelung potential due to atoms outside of the quantum cluster was represented by partial atomic charges located at the zeolite lattice sites. Using an approach recently proposed by Stefanovich and Troung [14], charges close to the quantum cluster are treated explicitly while the Madelung potential from the remaining charges from an infinite lattice is represented by a set of surface charges that were derived from the Surface Charge Representation of External Electrostatic Potential (SCREEP) method. More details on this method can be found elsewhere [15-16]. In this study, the total Madelung potential is represented by 1137 explicit charges and 146 surface charges. With this small number of point charges, additional computational cost is often less than 5% compared to bare cluster calculations.

Geometry optimizations were investigated with the density functional theory at the B3LYP/6-31G(d,p) level of theory using the GAUSSIAN 94 [17] program code. The computations were carried out using an IBM SP2 computer at KU Computing Center and a DEC Alphastation 250 and HP 9000/700 workstation at the Laboratory for Computational and Applied Chemistry (LCAC) at Kasetsart University.

3. RESULTS AND DISCUSSION

A series of model clusters of zeolite/$(H_2O)_n$; n = 1, 2, 3, and 4 are investigated at cluster and embedded cluster approaches. The fully optimized geometry strictures for all systems are documented in Tables 1-2. Adsorption energies evaluated by employing different models are given in Table 3.

3.1. One and two water molecules per acid site

Two representative cluster models of water adsorption on zeolites are investigated. In one of these, the hydrogen-bonded structures are stabilized on the Brønsted site. The other is a type of protonated model, in which hydronium ions forms two hydrogen bonds toward the unprotonated zeolite framework. All investigated models yielded only one minimum as hydrogen-bonded physisprobed water complexes, regardless of whether the initial framework structure had H_2O or H_3O^+. Similar findings to our results have just recently been reported by Sauer et. al. FT-IR [18-19] and ab initio [20] studies of water adsorption on zeolite support the direct clear evidence for the hydrogen bonded adsorption of water. Comparing the result between cluster and embedded cluster models, the Madelung potential has the effect of lengthening the O1-H1 bond distance (Brønsted acid site), and hence enhances the acidity of the Brønsted acid site (see Table 1).

The changes in the structural parameters of the zeolite upon complexation with water are minute but impressive. The results are in accordance with Gutmann's rules [21], i.e. a lengthening of the bridging O-H bond, a shortening of Al-O adjacent to this bond and a lengthening of Al-O (not adjacent to it).Similar trends are also observed for two water molecules per acid site. The O-H distance in the optimized structure of zeolite/H_2O and zeolite/$(H_2O)_2$ adducts (Fig.1-2) are evaluated to be 1.033 (1.045) and 1.043 (1.064) Å, respectively. The lengthened O-H distance of the latter model reflects an increase of the binding energy (see Table 3) (-15.99 (-17.42) versus –23.44 (-24.24) kcal/mol); values in

parenthesis are those obtained from the embedded cluster calculations. For cluster models, our findings agree closely with those reported by Zygmunt et al. [22], Gale [23], and Rice et al. [24] on the basis of DFT calculations carried out with a 3T, 4T, or a 5T cluster, respectively.

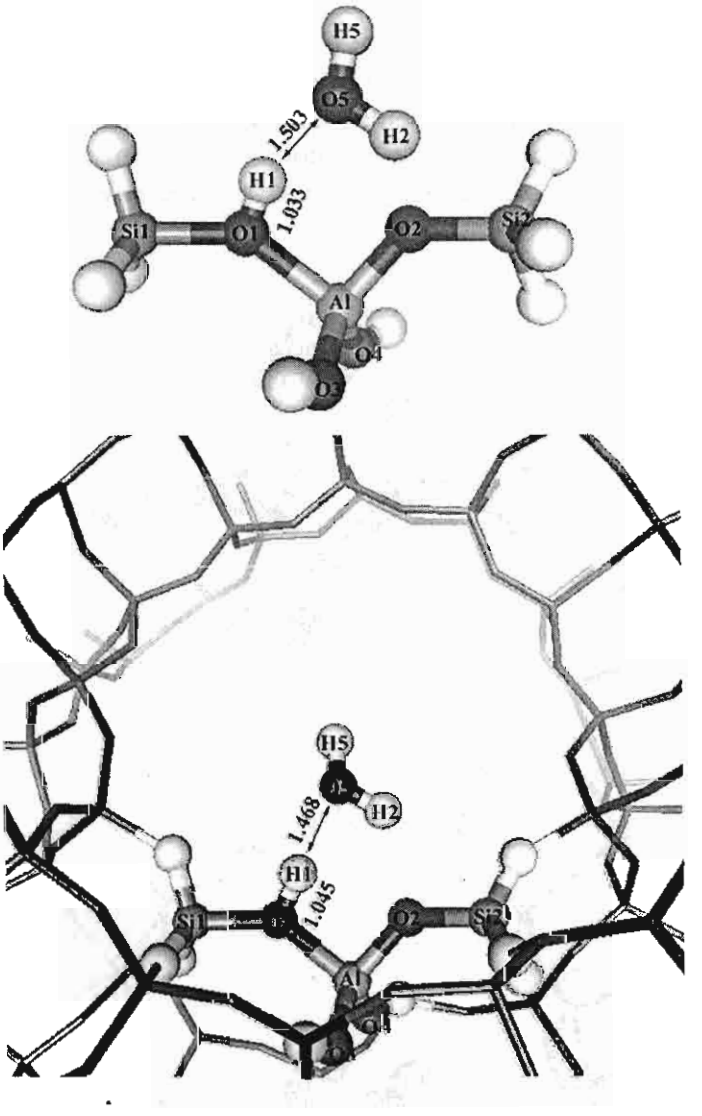

Fig. 1. Cluster and embedded cluster models of the faujasite/H_2O system. All values are given in angstroms.

The calculated adsorption energies and those estimated from the experimental values are different for the case of one adsorbed H_2O molecule but not for the adsorption of a second H_2O molecule. Since the uncertainties in the experimental adsorption energy values are not known [24], it is difficult to discuss this further.

Attempts have been made to observe the $Z^-/[H_3O]^+[H_2O]$, an initial structure in which a hydronium ion is optimized. The OH bond of H_3O^+ and the hydrogen bond angle (O-H...O) in the complex is constrained at the optimized H_3O^+ and 180° respectively.

However, during the optimization, the proton of H_3O^+ is transferred to the zeolite, and the final equilibrium complex H-Z/$[H_2O][H_2O]$ is obtained. The findings obtained from quantum cluster and embedded cluster models are consistent with those of Gale [23] and Rice et al. [24] that no evidence of proton transfer is observed with either one or two H_2O molecules adsorbed on the zeolitic cluster models. The experimentally observed reduction of adsorption energy per molecule when passing from one to two molecules per site of about 4.06 kcal/mol compares well with our predicted embedded value of 5.3 kcal/mol. We note that differences in cluster size, method of cluster termination, the presence or absence of structural constraints may contribute to the observed differences in the geometry.

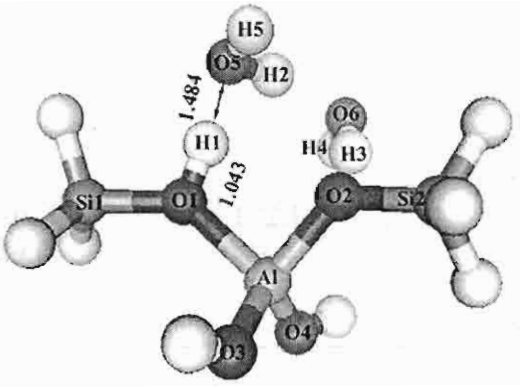

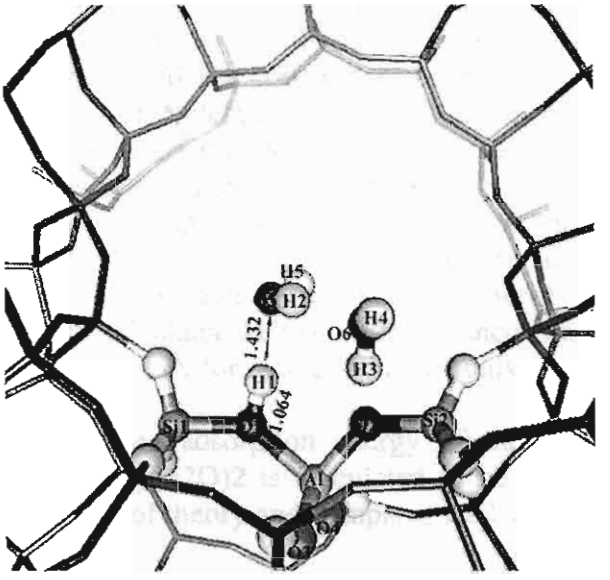

Fig. 2. Cluster and embedded cluster models of faujasite/$(H_2O)_2$ system. All values are given in angstroms.

Table 1
Structure parameters of the faujasite/water system.

Bond (Å) and angle (degree)	Faujasite/H2O		Faujasite/(H2O)2	
	Bare cluster	Embedded	Bare cluster	Embedded
	neutral	neutral	neutral	neutral
Al-O1	1.952	1.907	1.941	1.890
Al-O2	1.796	1.776	1.793	1.771
Al-O3	1.740	1.744	1.746	1.742
Al-O4	1.724	1.777	1.726	1.781
<Al-O>	1.803	1.801	1.801	1.796
O1-O5	2.523	2.507	2.521	2.494
O1-H1	1.033	1.045	1.043	1.064
O5-H1	1.503	1.468	1.484	1.432
O5-H5	0.967	0.968	0.998	0.968
O5-H2	0.996	0.982	0.967	0.999
O5-O6	-	-	2.634	2.603
O6-H3	-	-	0.986	0.975
O6-H4	-	-	0.965	0.966
O1-H1-O5	168.5	172.1	171.9	175.1
O2-Al-O1	89.9	93.4	90.2	93.9
O5-H5-O7	-	-	-	-
O5-H2-O6	-	-	158.8	154.3

3.2. Three and four water molecules per acid site

The results derived from the quantum cluster method indicate that the zeolitic proton remains non-transferred in the zeolite/(H2O)n n = 1-3 until at least four water molecules are solvated around the Brønsted acid site. For the embedded cluster method, the protonation seems certain when three water molecules are adsorbed on zeolite. It should be noted that there are many deviations between the isolated H3O+ structure and those for H3O+ in the zeolite/water complex. This observation is due mainly to the fact that the hydronium ion is stabilized by interacting with solvating water molecules and the anionic zeolite framework. The acid hydrogen sits 1.446 Å from the zeolitic framework oxygen and 1.067 Å from the oxygen of the H3O+ ion. The oxygen of the hydronium ion is located at 2.512 Å from the acid site oxygen O(1). This calculated H3O+....Oz distance can be compared well with the experimental observation of 2.51 Å for a weaker acid catalyst, silicoaluminosilicate (SAPO) [25].

The corresponding embedded adsorption energy of the high coverages of adsorption molecule of zeolite, ZO(H3O+)(H2O)2 is calculated to be −14.2 kcal/mol per molecule at B3LYP/6-31G++(2d, 2p) level of theory and compares well with experimental observation.

Table 2
Structure parameters of the faujasite/water system.

Bond (Å) and angle (degree)	Faujasite/$(H2O)_3$		Faujasite/$(H2O)_4$
	Bare cluster	Embedded	Bare cluster
	neutral	ion-pair	ion-pair
Al-O1	1.937	1.838	1.809
Al-O2	1.794	1.803	1.864
Al-O3	1.748	1.769	1.740
Al-O4	1.736	1.797	1.755
<Al-O>	1.804	1.802	1.792
O1-O5	2.468	2.512	2.726
O1-H1	1.090	1.446	1.813
O5-H1	1.381	1.067	0.987
O5-H5	0.982	0.999	0.984
O5-H2	0.993	1.026	1.441
O5-O6	2.653	2.542	2.480
O6-H3	0.987	0.983	1.069
O6-H4	0.966	0.972	0.996
O7-O5	2.790	2.692	2.759
O6-O8	-	-	2.680
O1-H1-O5	173.8	176.2	152.3
O2-Al-O1	90.4	95.3	92.9
O5-H5-O7	170.1	175.0	166.9
O5-H2-O6	160.7	167.2	166.1
O6-H4-O8	-	-	172.2

Table 3
Adsorption energies of water clusters on faujasite zeolite (kcal/mol per molecule).

FAU/ $(H2O)_n$	Bare Cluster				Embedded Cluster			
	B3LYP/6-31G(d,p)		B3LYP/6-311+G(d,p) //B3LYP/6-31G (d,p)		B3LYP/6-31G(d,p)		B3LYP/6-311+G (d,p) //B3LYP/ 6-31G (d,p)	
n	NC[a]	IP[b]	NC[a]	IP[b]	NC[a]	IP[b]	NC[a]	IP[b]
1	-20.92	-	-15.99	-	-22.41	-	-17.42	-
2	-17.02	-	-11.72	-	-17.52	-	-12.12	-
3	-14.14	-	-9.85	-	-	-19.57	-	-15.02
4	-	-13.92	-	-9.14	-	-	-	-

[a]NC = neutral complex. [b]IP = ion-pair complex

5. CONCLUSIONS

The influence of high coverages of adsorbing molecules on zeolites has been investigated by means of both the density functional theory quantum cluster and the embedded cluster methods. For cluster models, equilibrium structures determined for the adsorbing molecules successively added from one to four molecules per acid site. While

$[H_3SiOAl(OH)_2SiH_3]/[H_2O]$ and $[H_3SiOAl(OH)_2SiH_3]/[H_2O]_2$ are a hydrogen-bonded complex, cluster of $[H_3SiOAl(OH)_2SiH_3]/[H_2O]_4$ they contain both types of ion-pair and neutral complexes. The ion-pair complex results from a prompt and complete proton transfer from zeolite to adsorpbate that takes place in the high coverages. It is shown that for the zeolite $/(H_2O)_3$ complex, a complete proton transfer, $ZO(H_3O^+)$ $(H_2O)_2$, can be observed when the zeolite lattice potential is taken in to account.

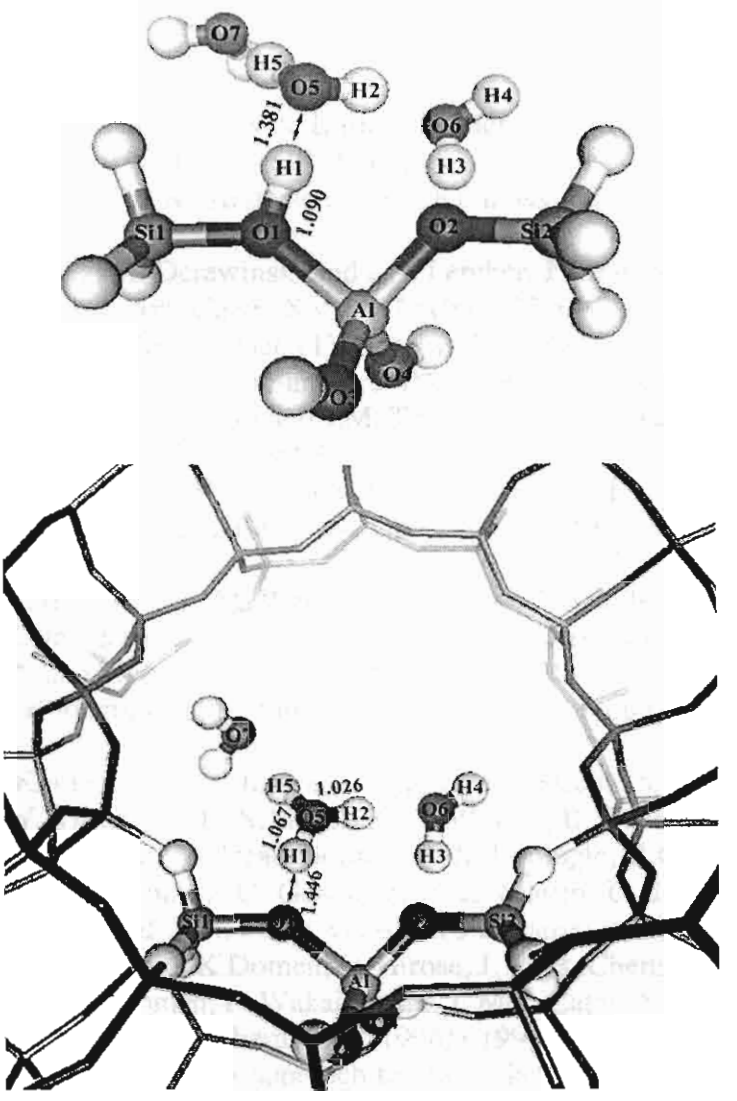

Fig. 3. Cluster and embedded cluster model of the faujasite/$(H_2O)_3$ system. All values are given in angstroms.

ACKNOWLEDGEMENTS

This work was supported by grants from the Thailand Research Fund (TRF) for supporting the basic research programme career development project and the Royal Golden Jubilee Ph.D. Programme to P.K. S.N. and S.J., as well as the Kasetsart University Research and Development Institute (KURDI) and The Ministry of University Affairs under the Science and Technology Higher Education Development Project (MUA-ADB funds).Our sincere thanks are due to Professors R. Ahlrichs (Karlsruhe, Germany) for his continued support of this work.

REFERENCES

1. S.P. Greatbanks, I.H. Hillier, and N.A. Burton, J. Chem. Phys., 105 (1996) 3370.
2. A. Ison and R.J. Gorte, J. Catal., 89 (1984) 150.
3. G. Mirth, J.A. Lercher, M.W. Anderson and J. Klinnoski, J. Chem. Soc. Faraday Trans, 86 (1990) 3039.
4. A. Jentys, G. Warecka, M. Derewinski and J.A. Lercher, J. Phys. Chem., 93 (1989) 4837.
5. F. Haase and J. Sauer, J. Am. Chem. Soc., 117 (1995) 3780.
6. S. Bates and J. Dwyer J. Mol. Struct. (Theochem), 306 (1994) 57.
7. A. G. Pelmenschikov and R.A. van Santen, J. Phys. Chem., 97 (1993) 10678.
8. L. Marchese, J. Chen, P.A. Wright and J.M. Thomas, J. Phys. Chem., 97 (1993) 8109.
9. J. Limtrakul, Chem. Phys., 193 (1995) 79.
10. E. Nusterer, P.E. Bloechl and K. Schwarz, Angew. Chem. Intern. Ed., 35 (1996) 175.
11. A. Kogelbauer, A.A. Nikolopoulos, J.G. Goodwin Jr. and G.Marcelin, J. Catal., 152 (1995) 122.
12. J. Limtrakul, P. Treesukol and M. Probst Chem. Phys., 215 (1997) 77-87.
13. W. J. mortier, E. van der Bosche, and J.B. Uytherhoven, Zeolites, 4 (1984) 41.
14. E. V. Stefanovich and Thanh N. Truong, J. Phys. Chem. B, 102 (1998) 3018.
15. J. Limtrakul, P. Khongpracha, S. Jungsuttivong and T.N. Troung, J. Mol. Catal. A, 153 (2000) 155.
16. J. Limtrakul, P. Khongpracha, S. Jungsuttivong, J. Mol. Strcut., 525 (2000) 155.
17. M. J. Frish, G. W. Trucks, H. B. Schlegel, P. M. W. Gill, B. G. Johnson, M. W. Wong, J. B. Foresman, M. A. Robb, M. Head-Gordon, E. S. Replogle, R.Gomperts, J. L. Andres, K. Raghavachari, I. S. Binkley, C. Gonzalez, R. L. Martin, D. J. Fox, D. J. DeFrees, J. Baker, J. J. P. Stewart and J. A. Pople, Gaussian 94, Gaussian, Pittsburgh,1994.
18. F. Wakabayashi, J.N. Kondo, K.Domen, C. Hirose, J. Phys .Chem., 100 (1996) 1442.
19. B. Lee, J.N. Kondo, K.Domen, F. Wakabayashi. J. Mol. Catal. A, 137 (1999) 269.
20. M .Krossner, J. Sauer, J. Phys. Chem., 100 (1996) 6199.
21. V. Gutmann, The donor-acceptor approach to molecular interactions, Plenum Press, New York 1978.
22. S.A. Zygmunt, L.A. Curtiss, L.E. Iton and M.K. Erhardt, J. Phys. Chem., 100 (1996) 6663.
23. J.D. Gale. Top. Catal., 3 (1996) 169.
24. M.J. Rice, A.K. Chakraborty and A.T. Bell, J. Phys. Chem A., 102 (1998) 7498.
25. L. Smith, A.K. Cheetham, R.E. Morris, L. Marchese, J.M. Thomas, P. A. Wright and J. Chen, Science, 271 (1996) 799-802.

VI.

Physical Organic Chemistry of solid catalysts

Hydrocarbon Transformation

- Chemical Physics Letters, 2001, 349, 161-166.

References and Notes

(1) Iwamoto, M.; Yahiro, H.; Tanda, K.; Mizuno, N.; Mine, Y.; Kagawa, S. J. Phys. Chem. 1991, 95, 3727.

(2) Sato, S.; Yoshihiro, Y.; Yahiro, H.; Mizuno, N.; Iwamoto, M. Appl. Catal. 1991, 70, L1.

(3) Shelef, M. Catal. Lett. 1992, 15, 305. (4) Li, Y. J.; Armor, J. N. Appl. Catal. 1991, 76, L1.

(5) Li, Y. J.; Hall, W. K. J. Catal. 1991, 129, 202. (6) Armor, J. N. Catal. Today 1997, 38, 163.

(7) Anpo, M.; Matsuoka, M.; Hanou, K.; Mishima, H.; Yamashita, H.; Patterson, H. H. Coord. Chem. ReV. 1998, 171, 175.

(8) Lamberti, C.; Salvalaggio, M.; Bordiga, S.; Geobaldo, F.; Spoto, G.; Zecchina, A.; Vlaic, G.; Bellatreccia, M. J. Phys. IV 1997, 7, 905.

(9) Lamberti, C.; Bordiga, S.; Salvalaggio, M.; Spoto, G.; Zecchina, A.; Geobaldo, F.; Vlaic, G.; Bellatreccia, M. J. Phys. Chem. B 1997, 101, 344.

(10) Bordiga, S.; Palomino, G. T.; Arduino, D.; Lamberti, C.; Zecchina, A.; Arean, C. O. J. Mol. Catal. A: Chem. 1999, 146, 97.

(11) Bordiga, S.; Lamberti, C.; Palomino, G. T.; Geobaldo, F.; Arduino, D.; Zecchina, A. Microporous Mesoporous Meter. 1999, 30, 129. (12) Dedecek, J.; Wichterlova, B. Phys. Chem. Chem. Phys. 1999, 1, 629.

(13) Arean, C. O.; Palomino, G. T.; Zecchina, A.; Spoto, G.; Bordiga, S.; Roy, P. Phys. Chem. Chem. Phys. 1999, 1, 4139.

(14) Arean, C. O.; Tsyganenko, A. A.; Platero, E. E.; Garrone, E.; Zecchina, A. Angew. Chem., Int. Ed. 1998, 37, 3161.

(15) Borovkov, V. Y.; Jiang, M.; Fu, Y. L. J. Phys. Chem. B 1999, 103, 5010.

(16) Kuroda, Y.; Kumashiro, R.; Yoshimoto, T.; Nagao, M. Phys. Chem. Chem. Phys. 1999, 1, 649.

(17) Kuroda, Y.; Mori, T.; Yoshikawa, Y.; Kittaka, S.; Kumashiro, R.; Nagao, M. Phys. Chem. Chem. Phys. 1999, 1, 3807.

(18) Trout, B. L.; Chakraborty, A. K.; Bell, A. T. J. Phys. Chem. 1996, 100, 17582.

(19) Liu, D. J.; Robota, H. J. Catal. Lett. 1993, 21, 291. (20) Dedecek, J.; Sobalik, Z.; Tvaruzkova, Z.; Kaucky, D.; Wichterlova, B. J. Phys. Chem. 1995, 99, 16327.

(21) Wichterlova, B.; Dedecek, J.; Vondrova, A. J. Phys. Chem. 1995, 99, 1065.

(22) Chen, L.; Chen, H. Y.; Lin, J.; Tan, K. L. Inorg. Chem. 1998, 37, 5294.

(23) Jang, H. J.; Hall, W. K.; Ditri, J. J. Phys. Chem. 1996, 100, 9416.

(24) Kuroda, Y.; Yoshikawa, Y.; Emura, S.; Kumashiro, R.; Nagao, M. J. Phys. Chem. B 1999, 103, 2155.

(25) Lamberti, C.; Spoto, G.; Scarano, D.; Paze, C.; Salvalaggio, M.; Bordiga, S.; Zecchina, A.; Palomino, G. T.; Dacapito, F. Chem. Phys. Lett.

1997, 269, 500.

(26) Schneider, W. F.; Hass, K. C.; Ramprasad, R.; Adams, J. B. J. Phys. Chem. 1996, 100, 6032.

(27) Brand, H. V.; Redondo, A.; Hay, P. J. J. Phys. Chem. B 1997, 101, 7691.

(28) Ramprasad, R.; Schneider, W. F.; Hass, K. C.; Adams, J. B. J. Phys. Chem. B 1997, 101, 1940.

(29) Hass, K. C.; Schneider, W. F. J. Phys. Chem. 1996, 100, 9292.

(30) Hass, K. C.; Schneider, W. F. Phys. Chem. Chem. Phys. 1999, 1, 639.

(31) Rice, M. J.; Chakraborty, A. K.; Bell, A. T. J. Phys. Chem. A 1998, 102, 7498.

(32) Schneider, W. F.; Hass, K. C.; Ramprasad, R.; Adams, J. B. J. Phys. Chem. B 1997, 101, 4353.

(33) Trout, B. L.; Chakraborty, A. K.; Bell, A. T. J. Phys. Chem. 1996, 100, 4173.

(34) Yokomichi, Y.; Yamabe, T.; Ohtsuka, H.; Kakumoto, T. J. Phys. Chem. 1996, 100, 14424.

(35) Zhanpeisov, N. U.; Matsuoka, M.; Mishima, H.; Yamashita, H.; Anpo, M. THEOCHEM J. Mol. Struct. 1998, 454, 201.

(36) Derouane, E. G.; Fripiat, J. G. Zeolites 1985, 5, 165.

(37) Alvaradoswaisgood, A. E.; Barr, M. K.; Hay, P. J.; Redondo, A. J. Phys. Chem. 1991, 95, 10031.

(38) Spoto, G.; Zecchina, A.; Bordiga, S.; Ricchiardi, G.; Martra, G.; Leofanti, G.; Petrini, G. Appl. Catal., B 1994, 3, 151.

(39) Nachtigallova, D.; Nachtigall, P.; Sierka, M.; Sauer, J. Phys. Chem. Chem. Phys. 1999, 1, 2019.

(40) Sarkany, J. J. Mol. Struct. 1997, 410, 145.

(41) Wichterlova, B.; Dedecek, J.; Sobalik, Z.; Vondrova, A.; Klier, K. J. Catal. 1997, 169, 194.

(42) Aylor, A. W.; Larsen, S. C.; Reimer, J. A.; Bell, A. T. J. Catal. 1995, 157, 592.

(43) Valyon, J.; Hall, W. K. J. Catal. 1993, 143, 520.

(44) Kanougi, T.; Tsuruya, H.; Oumi, Y.; Chatterjee, A.; Fahmi, A.; Kubo, M.; Miyamoto, A. Appl. Surf. Sci. 1998, 132, 561.

(45) Rodriguez-santiago, L.; Sierka, M.; Branchadell, V.; Sodupe, M.; Sauer, J. J. Am. Chem. Soc. 1998, 120, 1545.

(46) Schneider, W. F.; Hass, K. C.; Ramprasad, R.; Adams, J. B. J. Phys. Chem. B 1998, 102, 3692.

(47) Kobayashi, H.; Ohkubo, K. Appl. Surf. Sci. 1997, 121, 111. (48) Zhanpeisov, N. U.; Nakatsuji, H.; Hada, M.; Nakai, H.; Anpo, M. Catal. Lett. 1996, 42, 173.

(49) Civalleri, B.; Garrone, E.; Ugliengo, P. J. Phys. Chem. B 1998, 102, 2373.

(50) Blint, R. J. J. Phys. Chem. 1996, 100, 19518. (51) Kumashiro, R.; Kuroda, Y.; Nagao, M. J. Phys. Chem. B 1999, 103, 89.

(52) Cheung, T.; Bhargava, S. K.; Hobday, M.; Foger, K. J. Catal. 1996, 158, 301.

(53) Valyon, J.; Hall, W. K. J. Phys. Chem. 1993, 97, 1204.

(54) Brandle, M. S. Joachim; Dovesi, Roberto; Harrison, Nicholas M. J. Chem. Phys. 1998, 109, 10379.

(55) Civalleri, B.; Zicovich-Wilson, C. M.; Ugliengo, P.; Saunders, V. R.; Dovesi, R. Chem. Phys. Lett. 1998, 292, 394.

(56) Hill, J.-R. F.; Clive, M.; Delley, B. J. Phys. Chem. A 1999, 103, 3772.

(57) Kessi, A.; Delley, B. Int. J. Quantum Chem. 1998, 68, 135.

(58) Nicholas, J. B.; Hess, A. C. J. Am. Chem. Soc. 1994, 116, 5428.

(59) Shah, R.; Payne, M. C.; Lee, M. H.; Gale, J. D. Science 1996, 271, 1395.

(60) Stich, I.; Gale, J. D.; Terakura, K.; Payne, M. C. J. Am. Chem. Soc. 1999, 121, 3292.

(61) White, J. C.; Nicholas, J. B.; Hess, A. C. J. Phys. Chem. B 1997, 101, 590.

(62) Sherwood, P.; Devries, A. H.; Collins, S. J.; Greatbanks, S. P.; Burton, N. A.; Vincent, M. A.; Hillier, I. H. Faraday Discuss. 1997, 79.

(63) Greatbanks, S. P.; Hillier, I. H.; Sherwood, P. J. Comput. Chem. 1997, 18, 562.

(64) Stefanovich, E. V.; Truong, T. N. J. Phys. Chem. B 1998, 102, 3018.

(65) Vollmer, J. M.; Stefanovich, E. V.; Truong, T. N. J. Phys. Chem. B 1999, 103, 9415.

(66) Limtrakul, J.; Khongpracha, P.; Jungsuttiwong, S.; Truong, T. N. J. Mol. Catal. A: Chem. 2000, 153, 155.

(67) Sierka, M.; Sauer, J. Faraday Discuss. 1997, 41.

(68) Sierka, M.; Sauer, J. J. Mol. Graph Model 1998, 16, 274.

(69) Insight II Release 95.0; BIOSYM/MSI: San Diego, 1995.

(70) Ferrari, A. M.; Neyman, K. M.; Rosch, N. J. Phys. Chem. B 1997, 101, 9292.

(71) Frisch, M. J.; Trucks, G. W.; H. B. Schlegel, G. E. S.; Robb, M. A.; Cheeseman, J. R.; Zakrzewski, V. G.; Montgomery, J. A.; Stratmann, R. E.; Burant, J. C.; Dapprich, S.; Millam, J. M.; Daniels, A. D.; Kudin, K. N.; Strain, M. C.; Farkas, O.; Tomasi, J.; Barone, V.; Cossi, M.; Cammi, R.; Mennucci, B.; Pomelli, C.; Adamo, C.; Clifford, S.; Ochterski, J.; Petersson, G. A.; Ayala, P. Y.; Cui, Q.; Morokuma, K.; Malick, D. K.; Rabuck, A. D.; Raghavachari, K.; Foresman, J. B.; Cioslowski, J.; Ortiz, J. V.; Stefanov, B. B.; Liu, G.; Liashenko, A.; Piskorz, P.; Komaromi, I.; Gomperts, R.; Martin, R. L.; Fox, D. J.; Keith, T.; Al-Laham, M. A.; Peng, C. Y.; Nanayakkara, A.; Gonzalez, C.; Challacombe, M.; Gill, P. M. W.; Johnson, B. G.; Chen, W.; Wong, M. W.; Andres, J. L.; Head-Gordon, M.; Replogle, E. S.; Pople, J. A. Gaussian 98 (ReVision A.7); Pittsburgh, PA, 1998.

(72) Yamashita, H.; Matsuoka, M.; Tsuji, K.; Sioya, Y.; Anpo, M.; Che, M. J. Phys. Chem. 1996, 100, 397.

(73) Yamashita, H.; Matsuoka, M.; Anpo, M.; Che, M. J. Phys. IV 1997, 7, 941.

(74) Sengupta, D.; Schneider, W. F.; Hass, K. C.; Adams, J. B. Catal. Lett. 1999, 61, 179.

(75) Scarano, D.; Bordiga, S.; Lamberti, C.; Spoto, G.; Ricchiardi, G.; Zecchina, A.; Arean, C. O. Surf. Sci. 1998, 411, 272.

(76) Aylor, A. W. L.; Sarah, C.; Reimer, J. A.; Bell, A. T. J. Catal. 1995, 157, 592.

(77) Giamello, E.; D, M.; Magnacca, G.; Morterra, C.; Shioya, Y.; Nomura, T.; Anpo, M. J. Catal. 1992, 136, 510.

(78) Brand, H. V.; Redondo, A.; Hay, P. J. J. Mol. Catal. A: Chem. 1997, 121, 45.

(79) Tajima, N.; Hashimoto, M.; Toyama, F.; Elnahas, A. M.; Hirao, K. Phys. Chem. Chem. Phys. 1999, 1, 3823.

(80) Davydov, A. A. Zh. Fiz. Khim. 1991, 65, 269. 2428 J. Phys. Chem. B, Vol. 105, No. 12, 2001 Treesukol et al.

Output:

1. International Publications:

(1) P. Treesukol, T.N. Truong and J. Limtrakul*, Adsorption of NO_x and CO on Cu (I)-ZSM-5: A clsuter and embeded cluster study, ***Journal of Physical Chemistry: B*** 105 (2001) 2421-2428.

(2) J. Limtrakul*, S. Nokbin and P. Chichay. Proton dynamics in high coverages of zeolite/water, ***Journal of Molecular Structure*** 560 (2001) 169-177.

(3) J. Limtrakul*, S. Jungsuttiwong, P. Khongpracha P. Chichay and S. Nokbin. The effect of high coverage of faujasite/water sysytem: a density functional embedded cluster approach. ***Studies in Surface Science and Catalysis*** 135 (2001) 2469-2476.

(4) S. Jungsuttiwong, P. Khongpracha, and J. Limtrakul*Ag-carbonyl complex: A comparison to Cu-carbonyl complex, ***Studies in Surface Science and Catalysis*** 135 (2001) 2518-2525

(5) P. Treesukol, J. Limtrakul and T.N. Truong. A full quantum embedded cluster methodology: application to proton sitting in Chabazite ***Chemical Physics Letters, 350 (2001) 128-134.***

(6) J. Limtrakul, T. Nanok, S. Jungsuttiwong and T.N. Truong. Adsorption of unsaturated hydrocarbons on zeolites: The Effect of the zeolite framework on adsorption properties. ***Chemical Physics Letters, 349 (2001) 161-166.***

(7) J. Limtrakul, S. Jungsuttiwong, P. Khongpracha and T. N. Truong, Adsorption of carbon monoxide in H-ZSM-5 and Li-ZSM-5 zeolites: an embedded ab initio clusters study. ***Journal of Molecular Catalysis A*** 153 (2000) 155-163.

(8) J. Limtrakul, S. Jungsuttiwong and P. Khongpracha, Adsorption of carbon monoxide on H-FAU and Li-FAU zeolites: an embedded cluster approach, ***Journal of Molecular Structure*** 525 (2000) 153-162.

(9) J. Limtrakul and M. Kuno, The interactions of sorbates with gallosilicates and alkali-metal exchanged gallosilicates. ***Journal of Molecular Structure*** 510 (1999) 131-147..

2. การนำผลงานวิจัยไปใช้ประโยชน์

เชิงสาธารณะ

มีเครือค่ายความร่วมมือกับ *Chemistry Department University of Utah* ภาควิชาเคมี สถาบันเทคโนโลยีพระจอมเกล้าเจ้าคุณทหารลาดกระบัง และภาควิชาวิศวกรรมเคมี คณะวิศวกรรม มหาวิทยาลัยเกษตรศาสตร์

เชิงวิชาการ

ผลิตนิสิตปริญญาโทและเอก โดยมีนิสิตที่กำลังศึกษาปริญญาโท 6 คน และปริญญาเอก 5 คน และมีนิสิตสำเร็จปริญญาโทจำนวน 1 คน

3. International Conference Proceedings:

(1) Limtrakul*, J. Nokbin, S., Khongpracha P., Jungsuttiwong S. "High coverages effect on proton transfer of faujasite/water system: density function embedded cluster approach" 13th International Zeolite Chemistry and Catalysis, Montpelier, France.

(2) Treesukol, P., Limtrakul*, J., and Truong, T.N. (2000) "Embedded cluster study of adsorption of nitrogen monoxide and carbon monoxide on copper exchanged ZSM-5" West Coast Theoretical Chemistry Conference, June 26-28, 2000, University of Utah, UT

(3) Treesukol, P.and Limtrakul*, J. "The interaction of methanol with petrochemical catalyst: A new ab initio embedded cluster method" Anaheim (1999), American Chemical Society, National meeting, Anaheim, California, USA.

(4) Jungsuttiwong S., Khongpracha P., and Limtrakul, J. "A theoretical study of adsorption of carbon monoxide on Ag-ZSM-5 zeolite" 13th International Zeolite Chemistry and Catalysis, Montpelier, France.

National Conference Proceedings:

(1) Nokbin, S., Chuichay, P., and Limtrakul, J. (2000) "Adsorption process of water cluster on faujasite catalyst" 26th Congress on science and technology of Thailand, October 18-20, 2000

(2) Inntam, C. and Limtrakul, J. (2000) New cluster model of catalytically active site in Ti-silica catalyst" 26th Congress on science and technology of Thailand, October 18-20, 2000

(3) Jungsuttiwong, S., Kongpracha, P., and Limtrakul, J. (2000) "Carbonyl complexes in Ag+-ZSM-5: A comparison with Cu+-ZSM-5" 26th Congress on science and technology of Thailand, October 18-20, 2000

(4) Kongpracha, P., Jungsuttiwong, S., and Limtrakul, J. (2000) "A new methodology for accurate and effective in incorporating electrostatic potential into embedded cluster model of zeolite cage" 26th Congress on science and technology of Thailand, October 18-20, 2000

(5) Kanokthip and Jumras Limtrakul "Density functional theory study of platinum mobility in zeolitic catalyst" 27th Congress on science and technology of Thailand, October 16-18, 2001.

(6) Tanin Nanok and Jumras Limtrakul "Potential energy surface of ethylene reaction on zeolites: the embedded quantum cluster study" 27th Congress on science and technology of Thailand, October 16-18, 2001.

(7) Sombat Ketrat and Jumras Limtrakul "Adsorption of oxygen, nitrogen and ethylene on silver-exchanged ZSM-5" 27th Congress on science and technology of Thailand, October 16-18, 2001.

(8) Virasak Dungsrikaew, Jakkapan Sirijaraensre and Jumras Limtrakul
"Effective and accurate method of ab initio embedded cluster calculation of crystals and macromolecules" 27th Congress on science and technology of Thailand, October 16-18, 2001.

(9) Jakkapan Sirijaraensre and Jumras Limtrakul
"Electronic embedded cluster study of Beckmannn rearrangement mechanisms on ZSM-5 catalyst" 27th Congress on science and technology of Thailand, October 16-18, 2001.

(10) Chan Inntam and Jumras Limtrakul
"Density funtional theory study on the ethylene epoxidation over Ti-silicalite (TS-1): cluster and embedded cluster approach" 27th Congress on science and technology of Thailand, October 16-18, 2001.

(11) Somkiat Nokbin and Jumras Limtrakul
"High loadings of CH_3OH on Faujasitic petrochemical catalysts: an electronic cluster study" 27th Congress on science and technology of Thailand, October 16-18, 2001